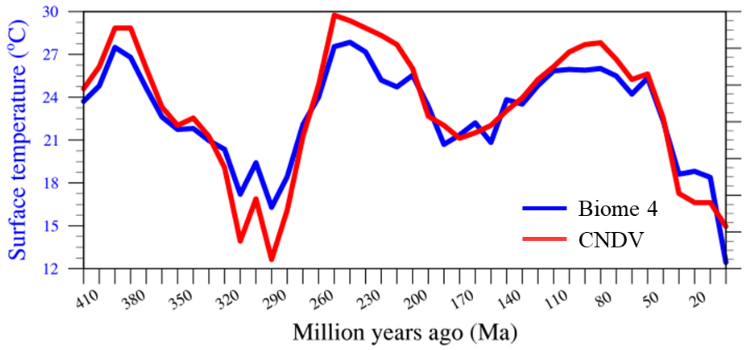

Figure S1. The evolution of simulated GMSTs under identical atmospheric CO_2 forcing using the CNDV vegetation module (red line) and the BIOME4 vegetation module (blue line). The prescribed deep-time CO_2 forcing is derived from Li et al. (2022).

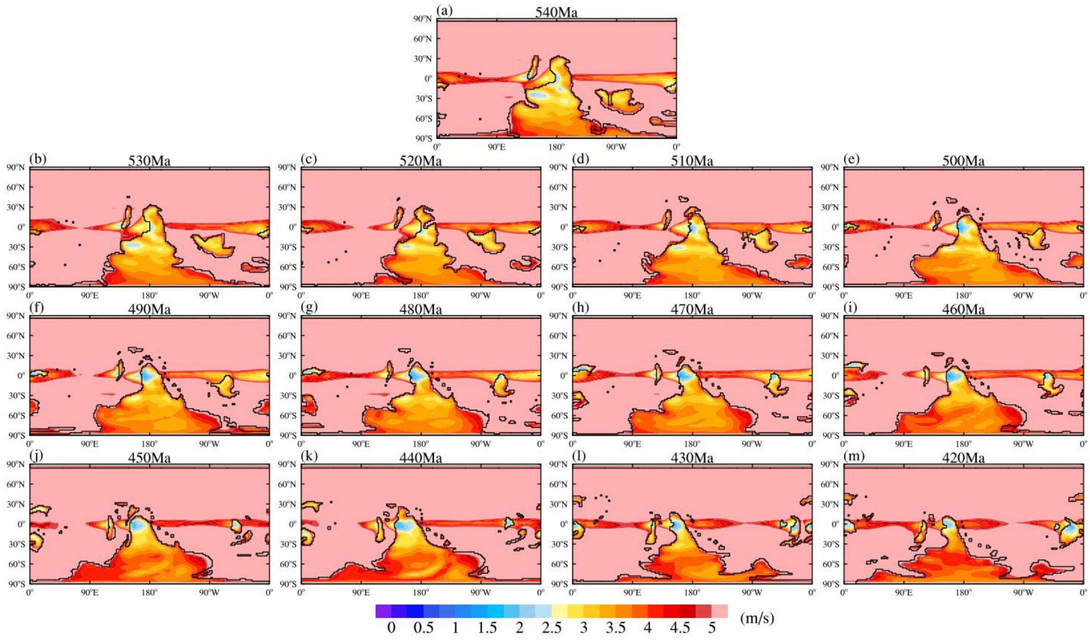

Figure S2. Annual-mean 10 m wind speed (m/s) for 540 Ma to 420Ma.

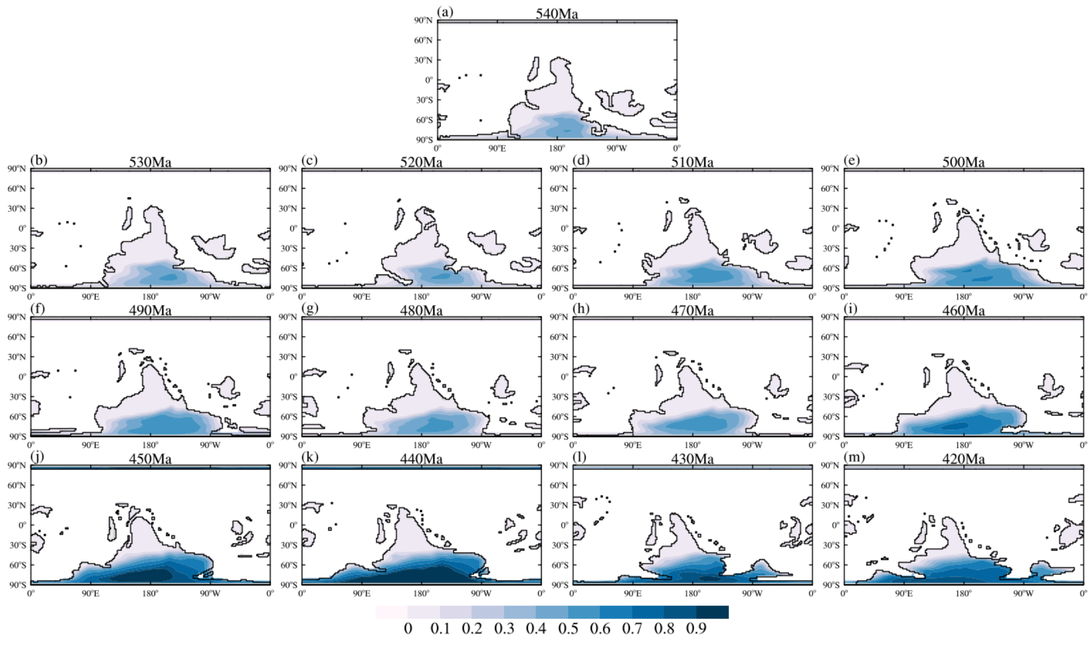

Figure S3. Annual-mean fraction of ground covered by snow for 540 Ma to 420Ma.

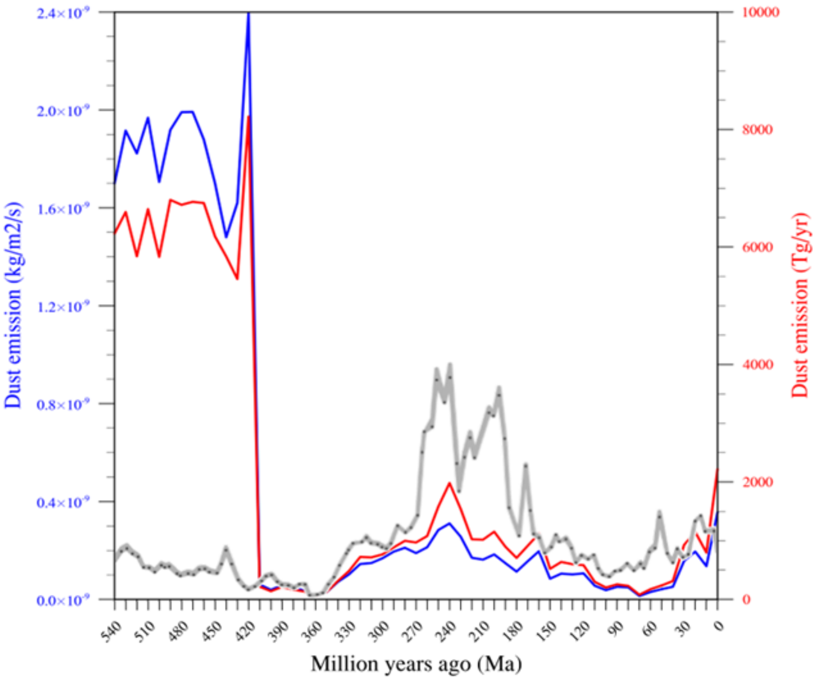

Figure S4. Global dust emission in this work (blue line in kg/m^2/s, red line in Tg/yr) and in Xie et al. (2024) (grey shading in kg/m^2/s).

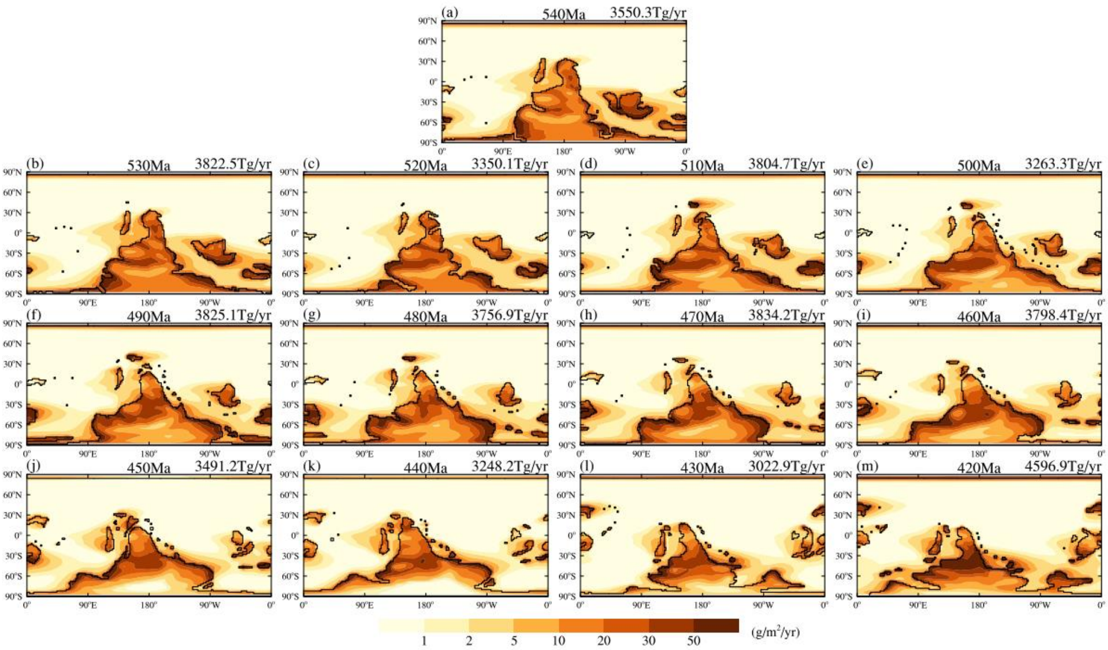

Figure S5. Annual-mean dust dry deposition (g/m^2/yr) for 540 Ma to 420Ma.

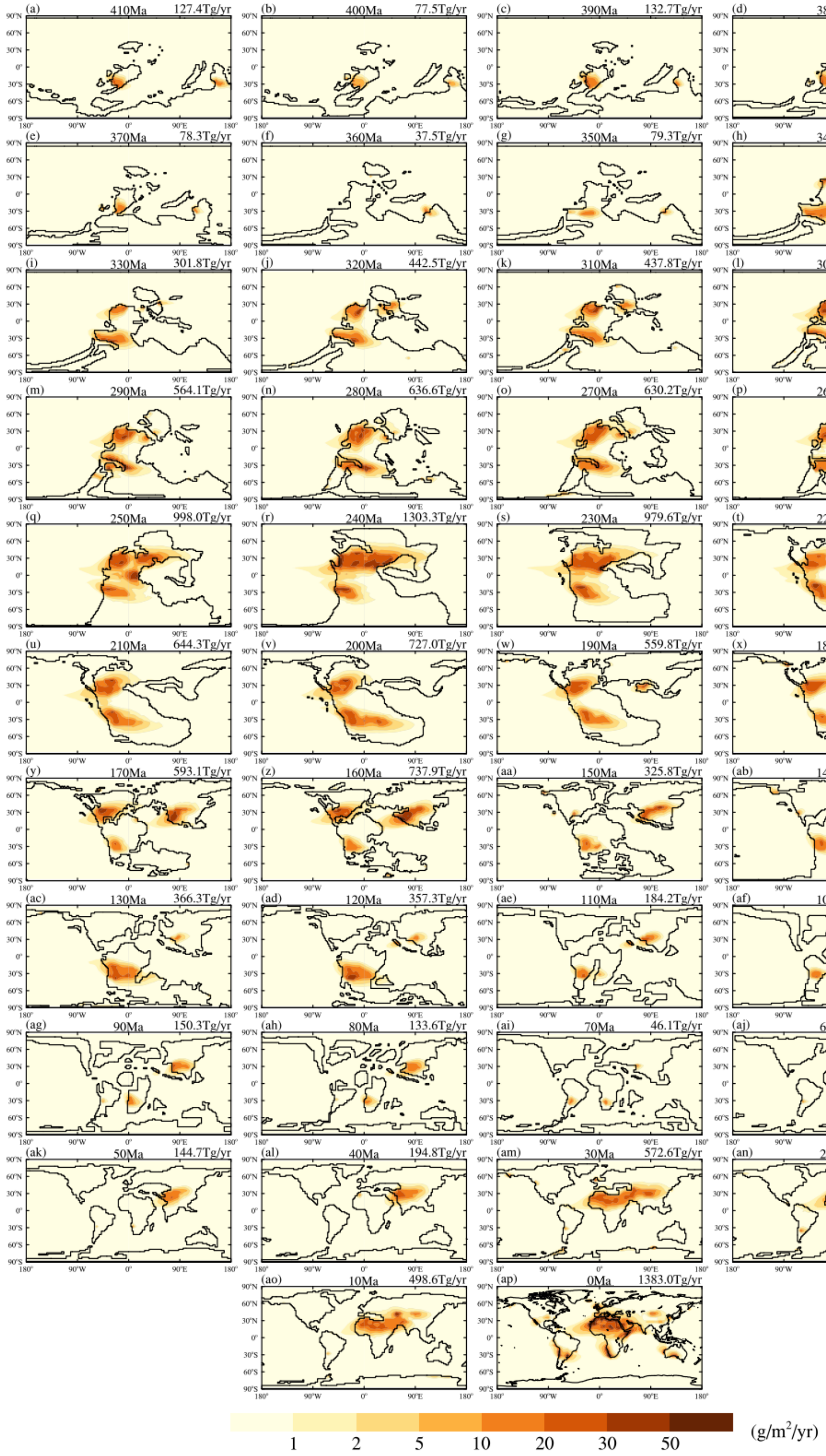

Figure S6. Annual-mean dust dry deposition (g/m^2/yr) for 410 Ma to 0 Ma.

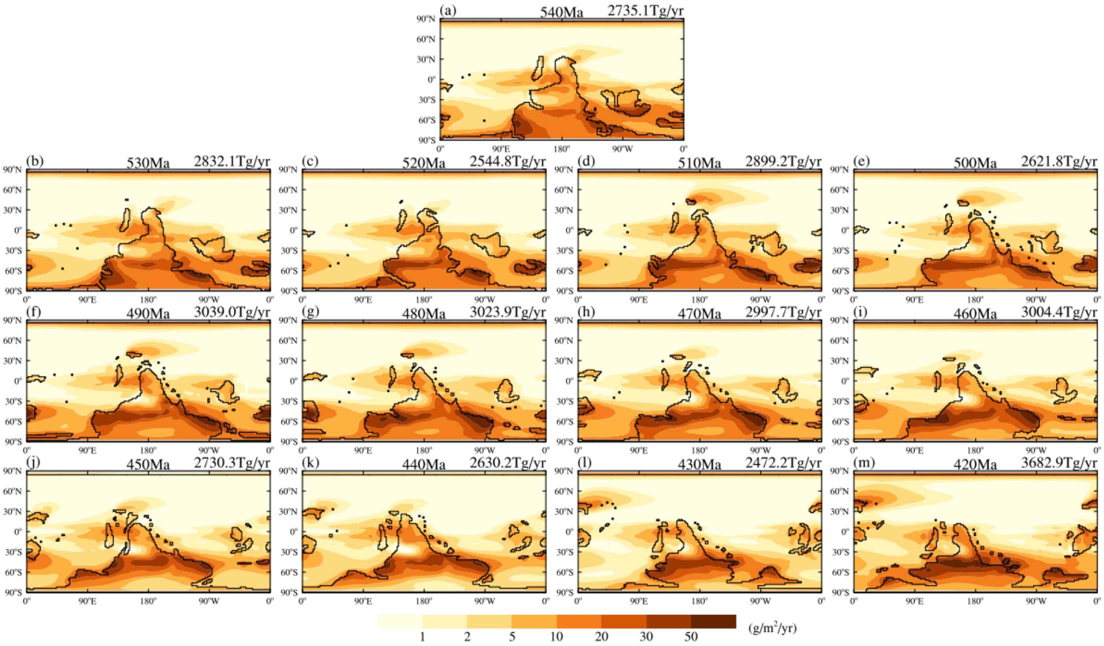

Figure S7. Annual-mean dust wet deposition (g/m^2/yr) for 540 Ma to 420Ma.

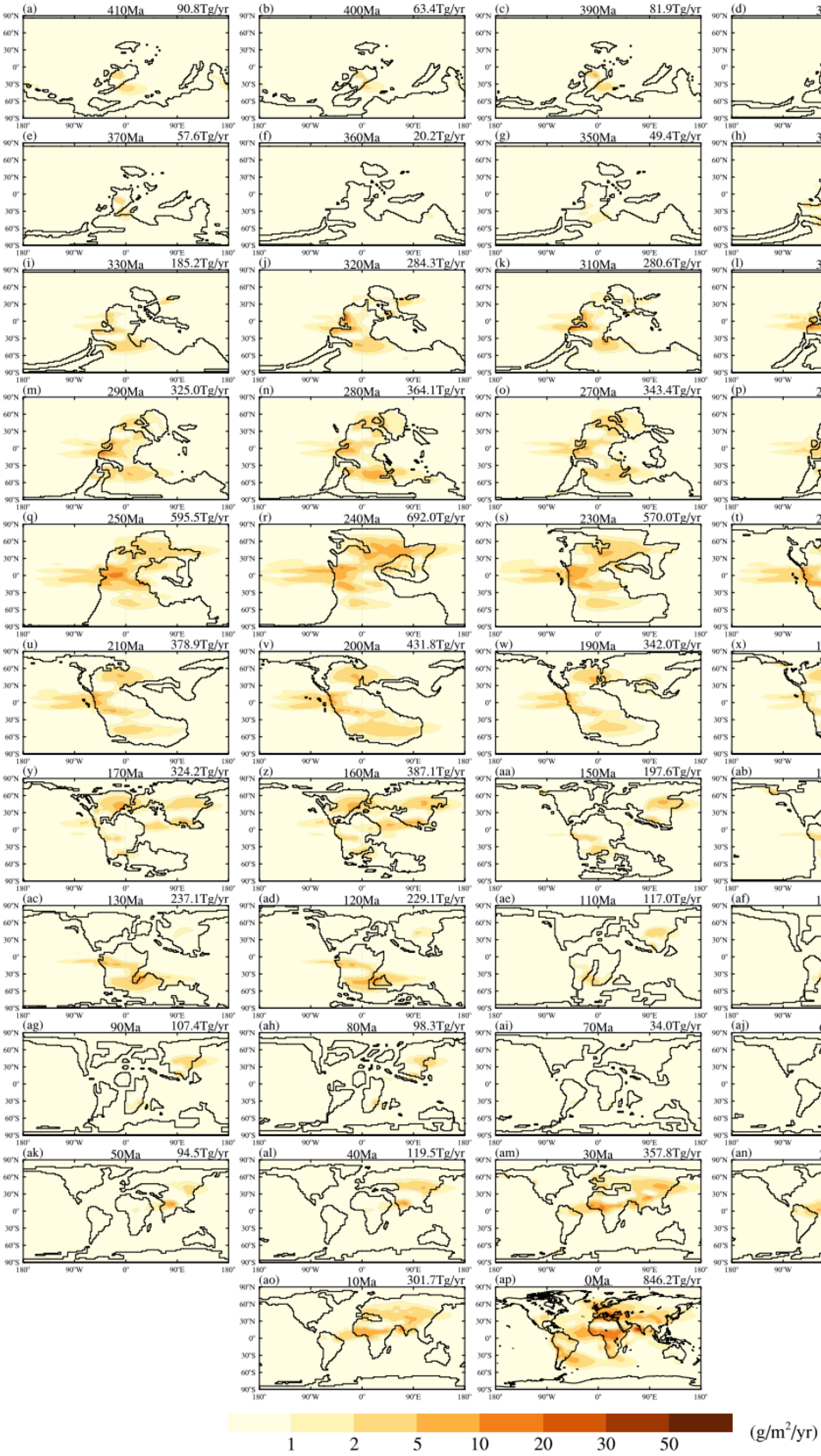

Figure S8. Annual-mean dust wet deposition ($g/m^2/yr$) for 410 Ma to 0 Ma.

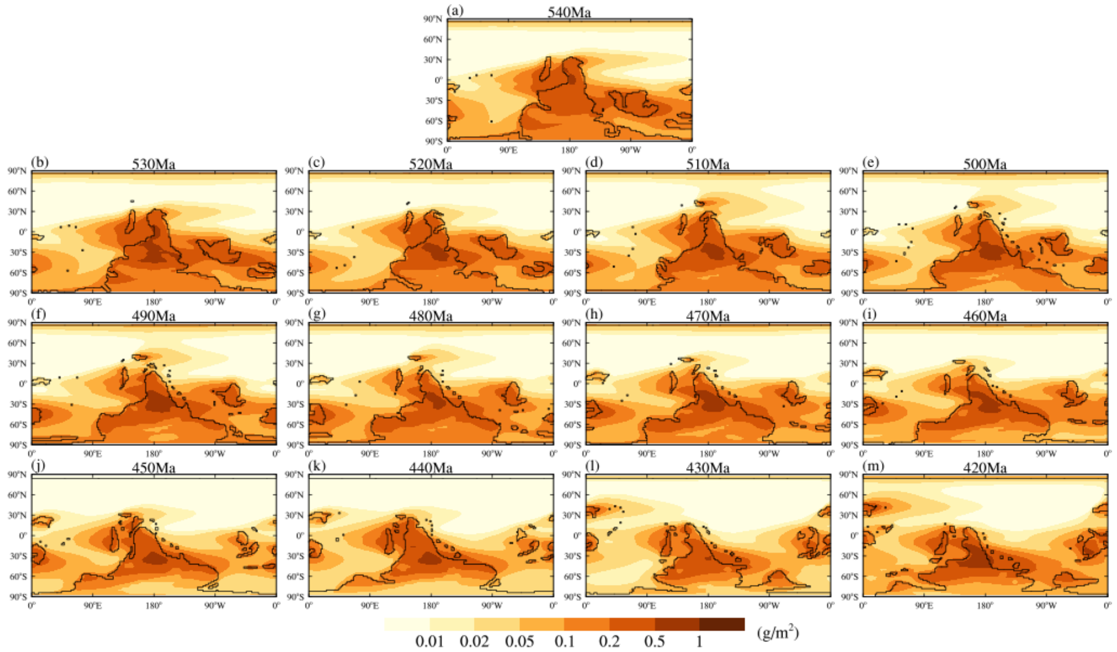

Figure S9. Annual-mean dust loading (g/m^2) for 540 Ma-420Ma.

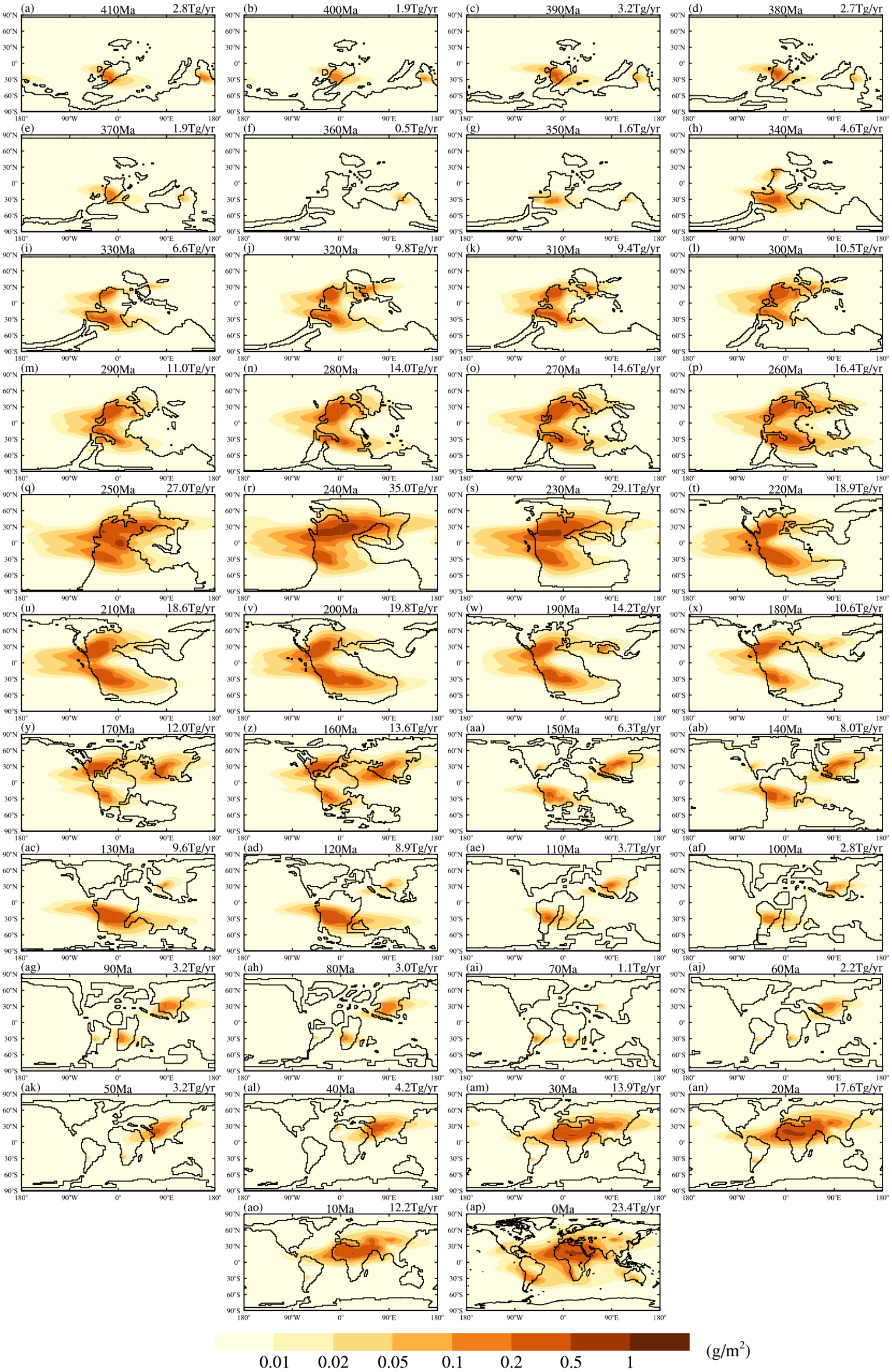

Figure S10. Annual-mean dust loading (g/m^2) for 410 Ma to 0 Ma.

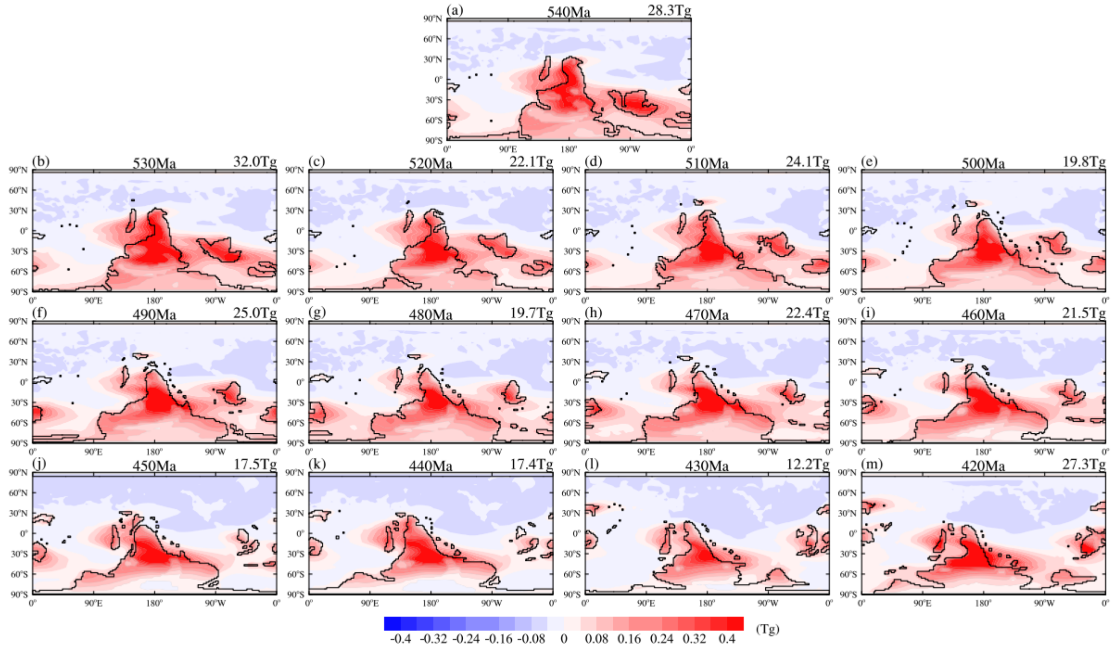

Figure S11. The differences in dust loading (Tg) between DUST2 experiments and DUST1 experiments for 540 Ma to 420Ma.

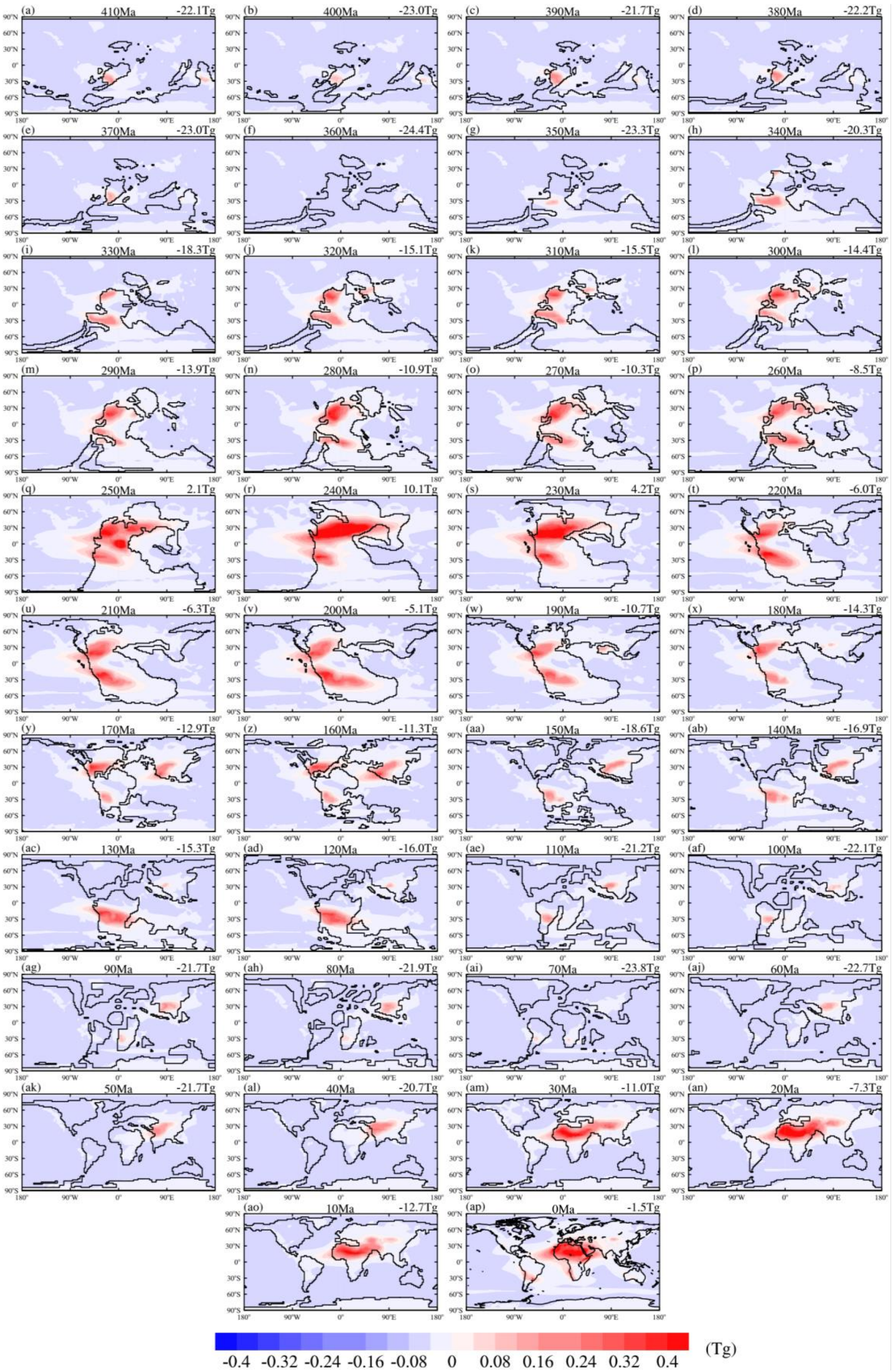

Figure S12. The differences in dust loading (Tg) between DUST2 experiments and DUST1 experiments for 410 Ma to 0 Ma.

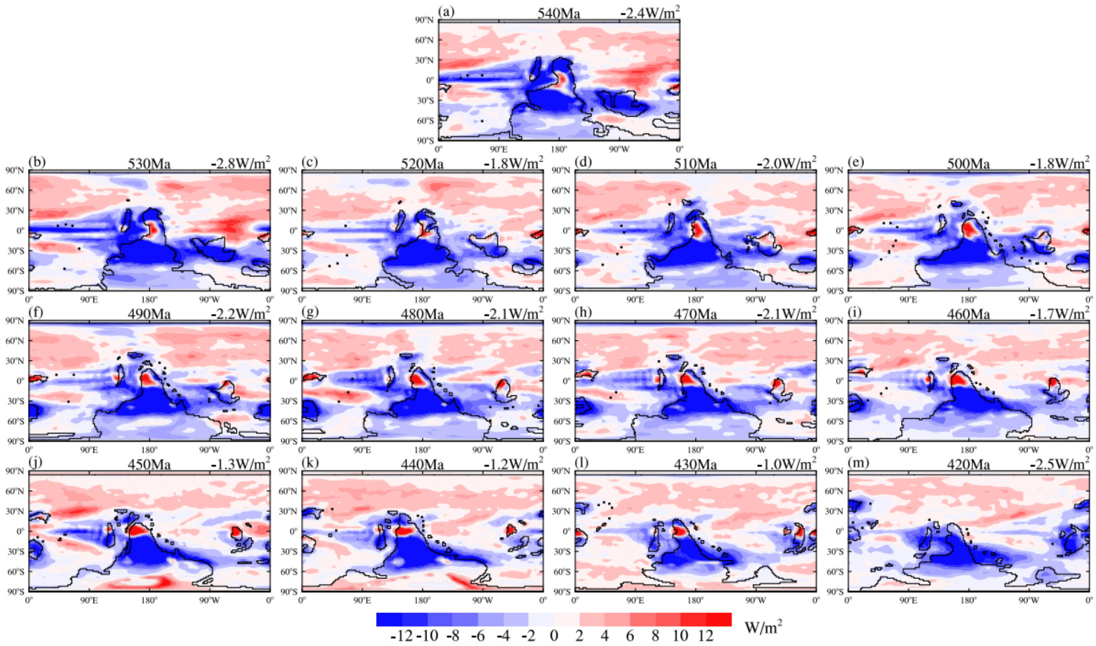

Figure S13. The differences in surface downwelling solar radiation (W/m^2) between DUST2 experiments and DUST1 experiments for 540 Ma to 420Ma.

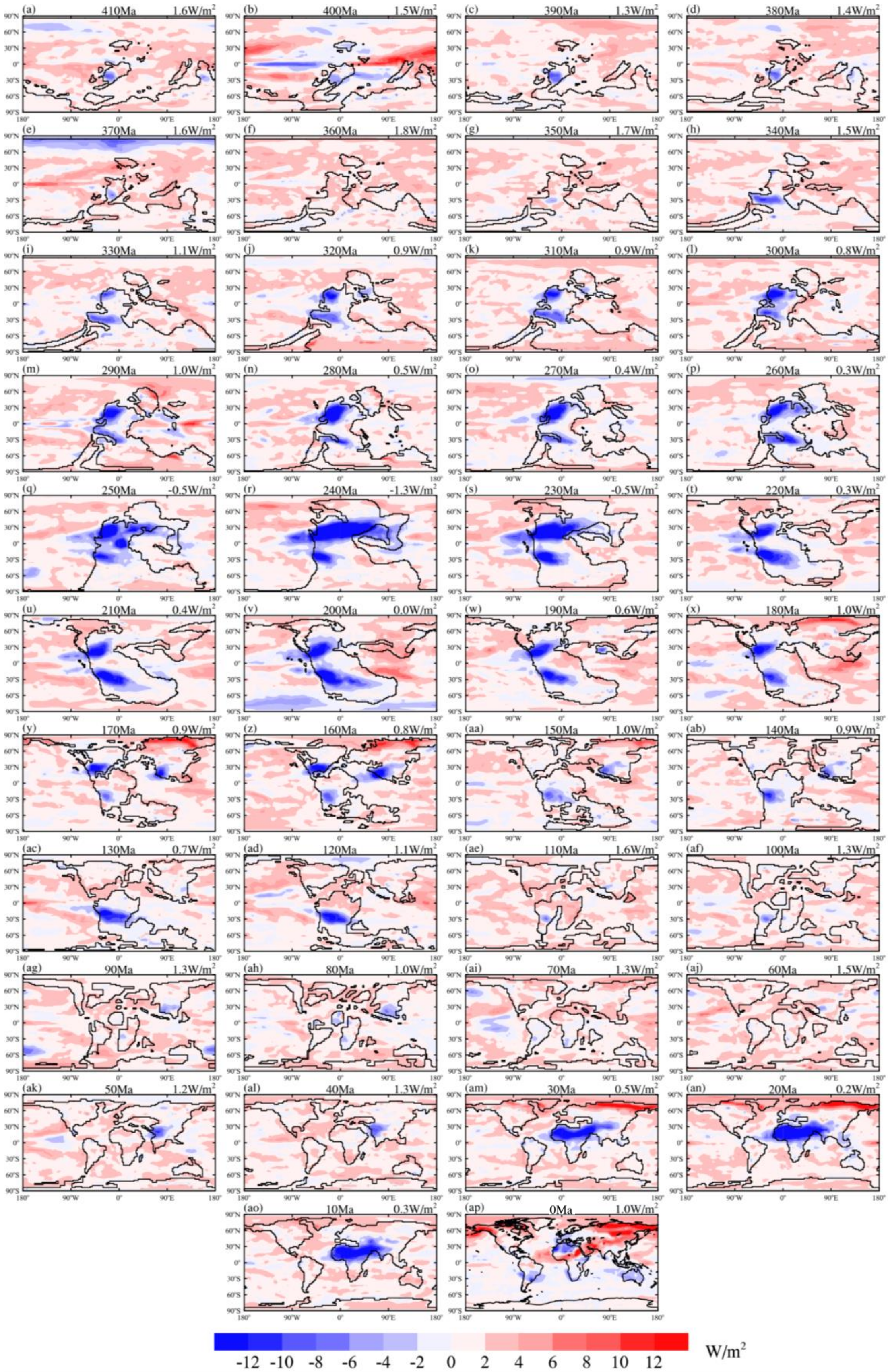

Figure S14. The differences in surface downwelling solar radiation (W/m^2) between DUST2 experiments and DUST1 experiments for 410 Ma to 0 Ma.

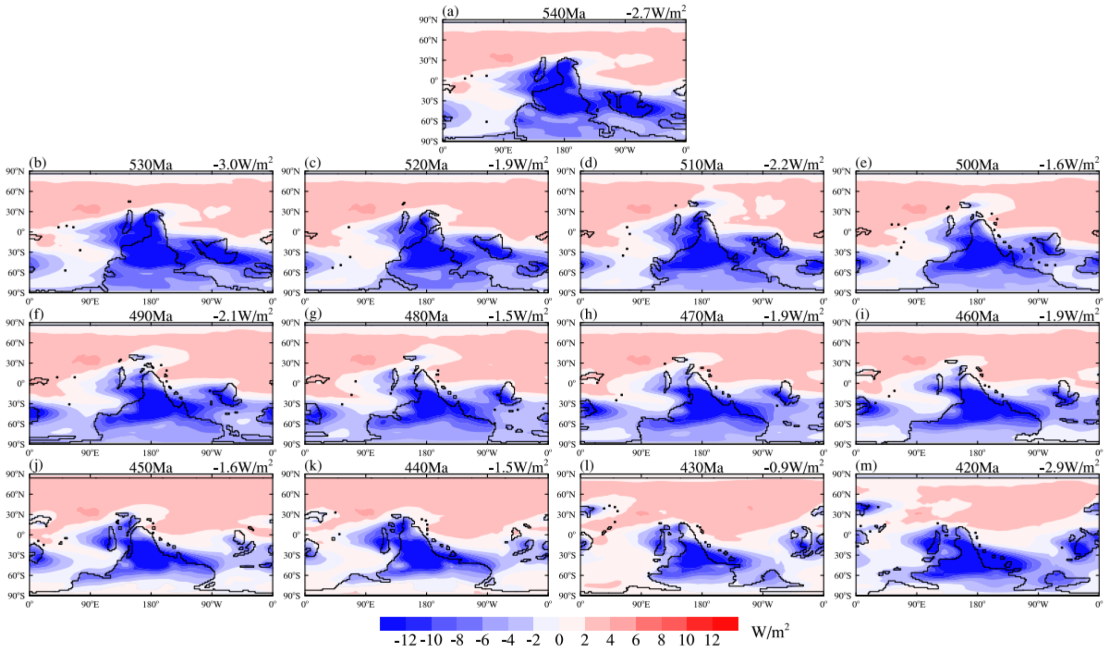

Figure S15. The differences in clear-sky downwelling solar radiation at the surface (W/m^2) between DUST2 experiments and DUST1 experiments for 540 Ma to 420Ma.

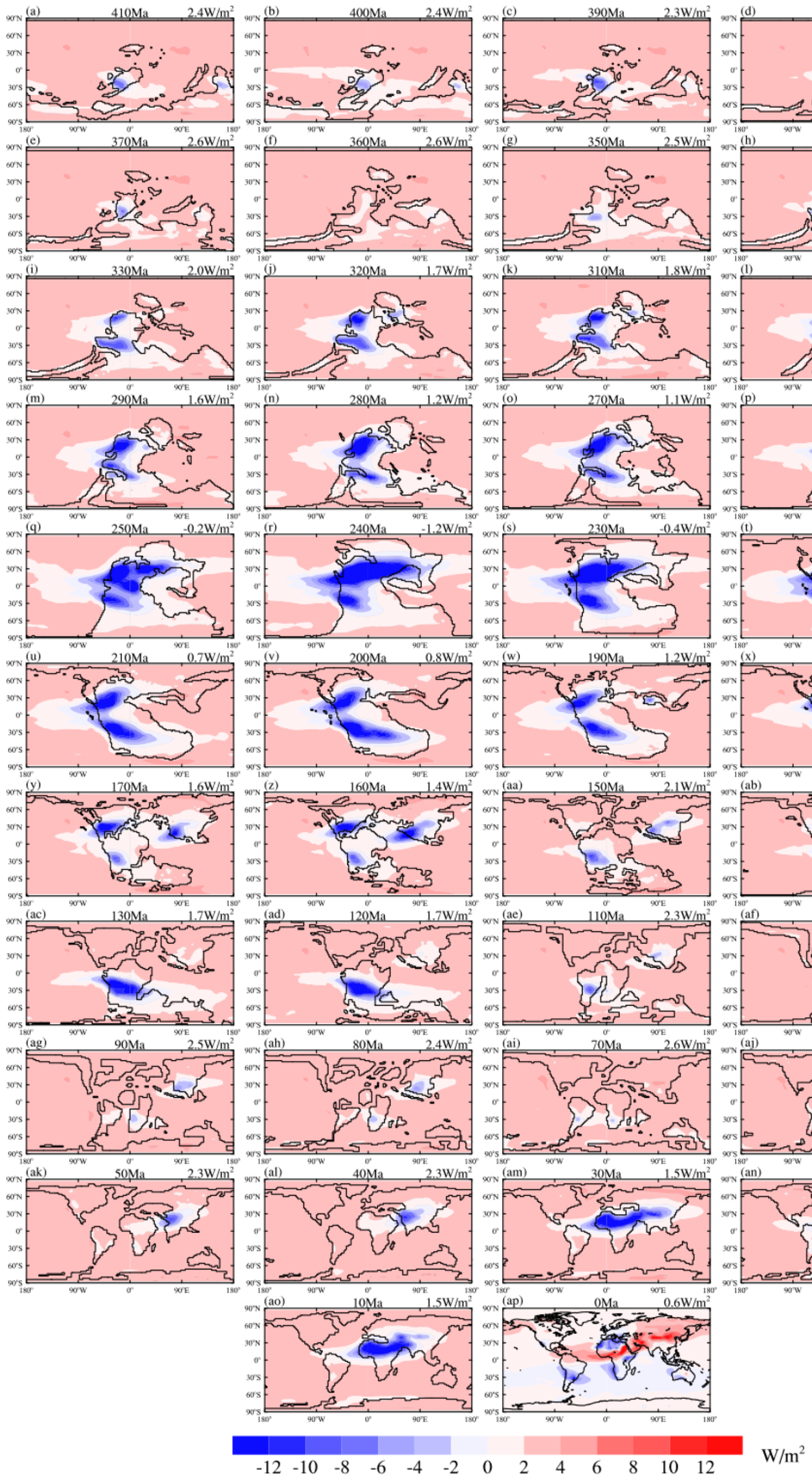

Figure S16. The differences in clear-sky downwelling solar radiation at the surface (W/m^2) between DUST2 experiments and DUST1 experiments for 420 Ma to 0 Ma.

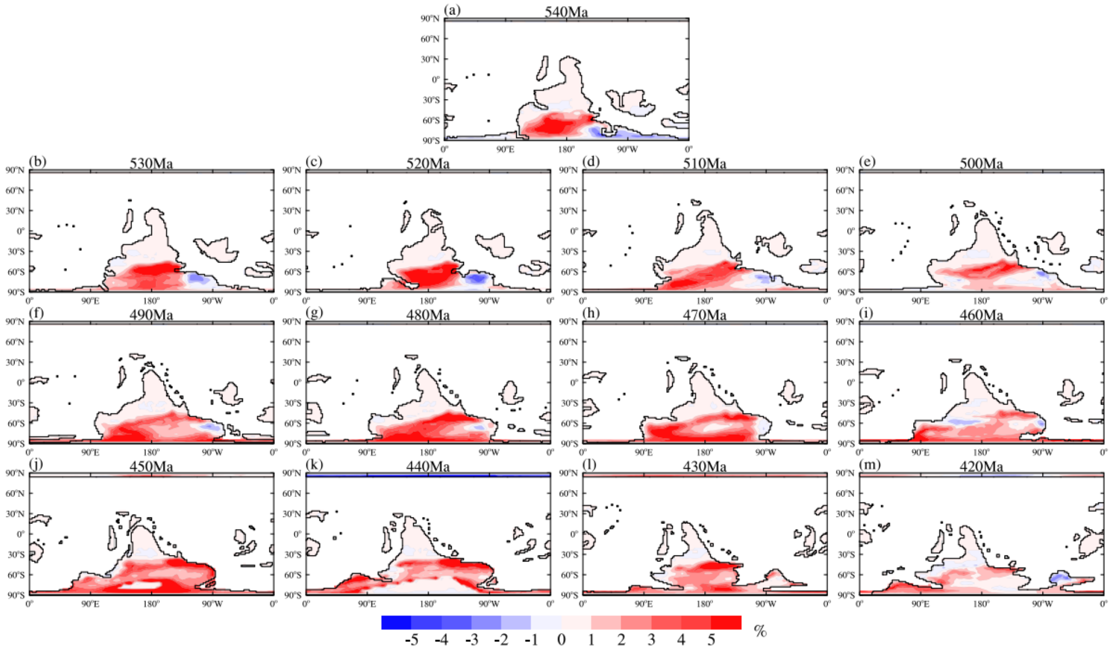

Figure S17. The differences of fraction of ground covered by snow (%) between DUST2 experiments and DUST1 experiments for 540 Ma to 420 Ma.

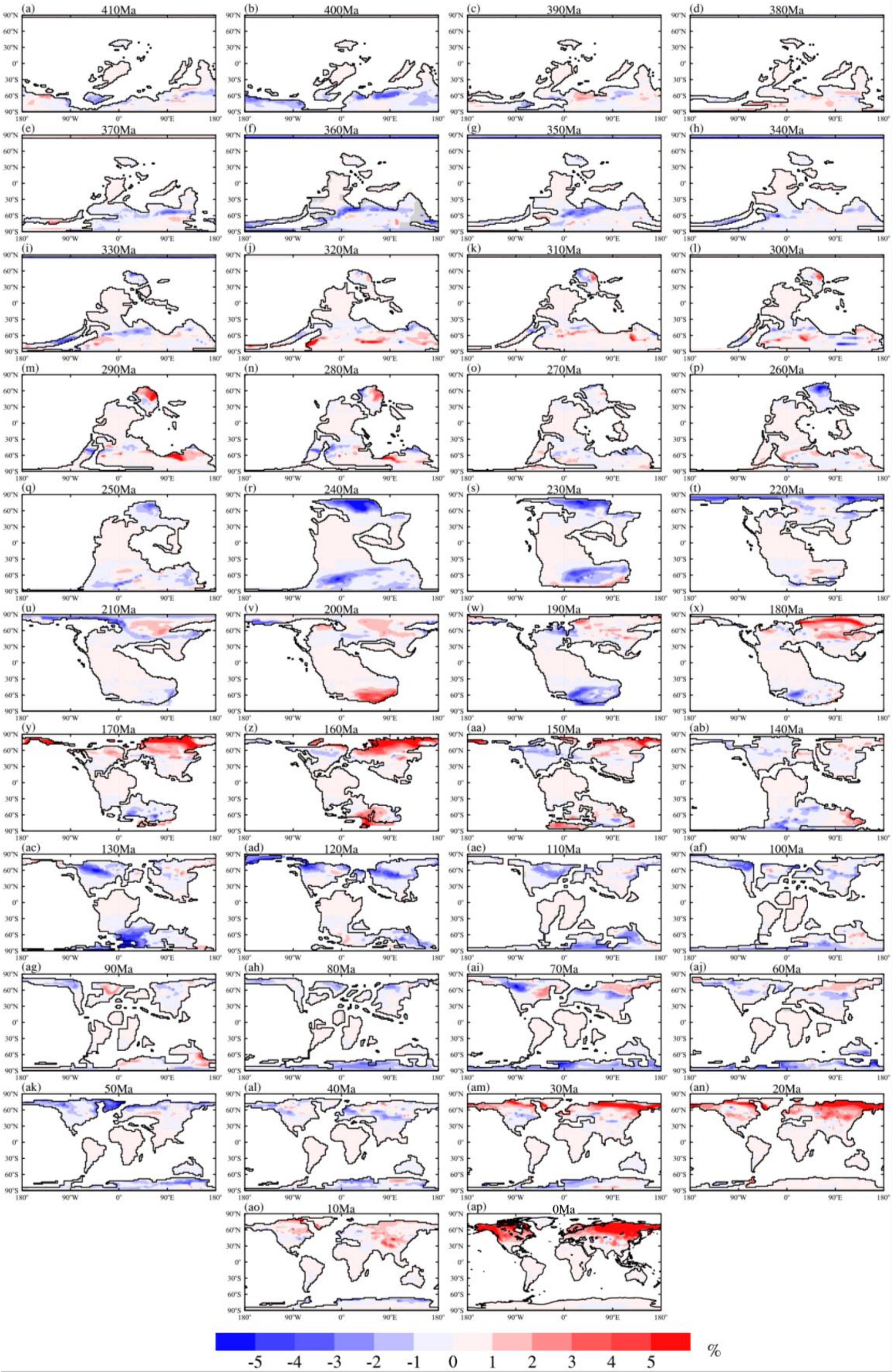

Figure S18. The differences of fraction of ground covered by snow (%) between DUST2 experiments and DUST1 experiments for 410 Ma to 0 Ma.

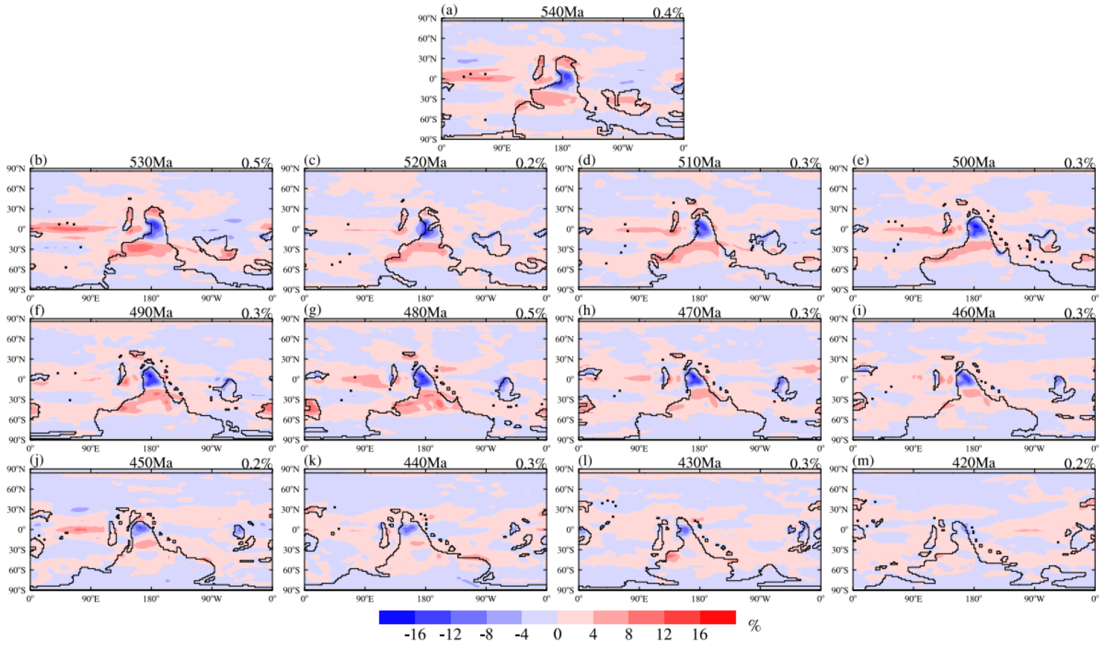

Figure S19. The differences of vertically-integrated total cloud fraction (%) between DUST2 experiments and DUST1 experiments for 540 Ma to 420 Ma.

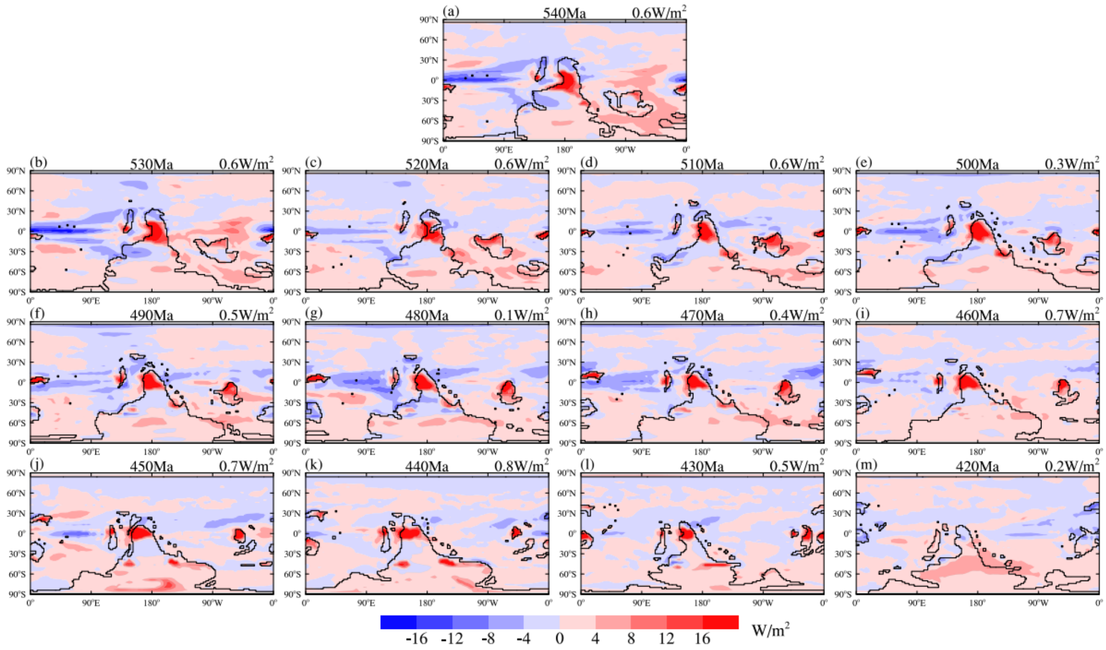

Figure S20. The differences of shortwave cloud forcing (W/m^2) between DUST2 experiments and DUST1 experiments for 540 Ma to 420 Ma.

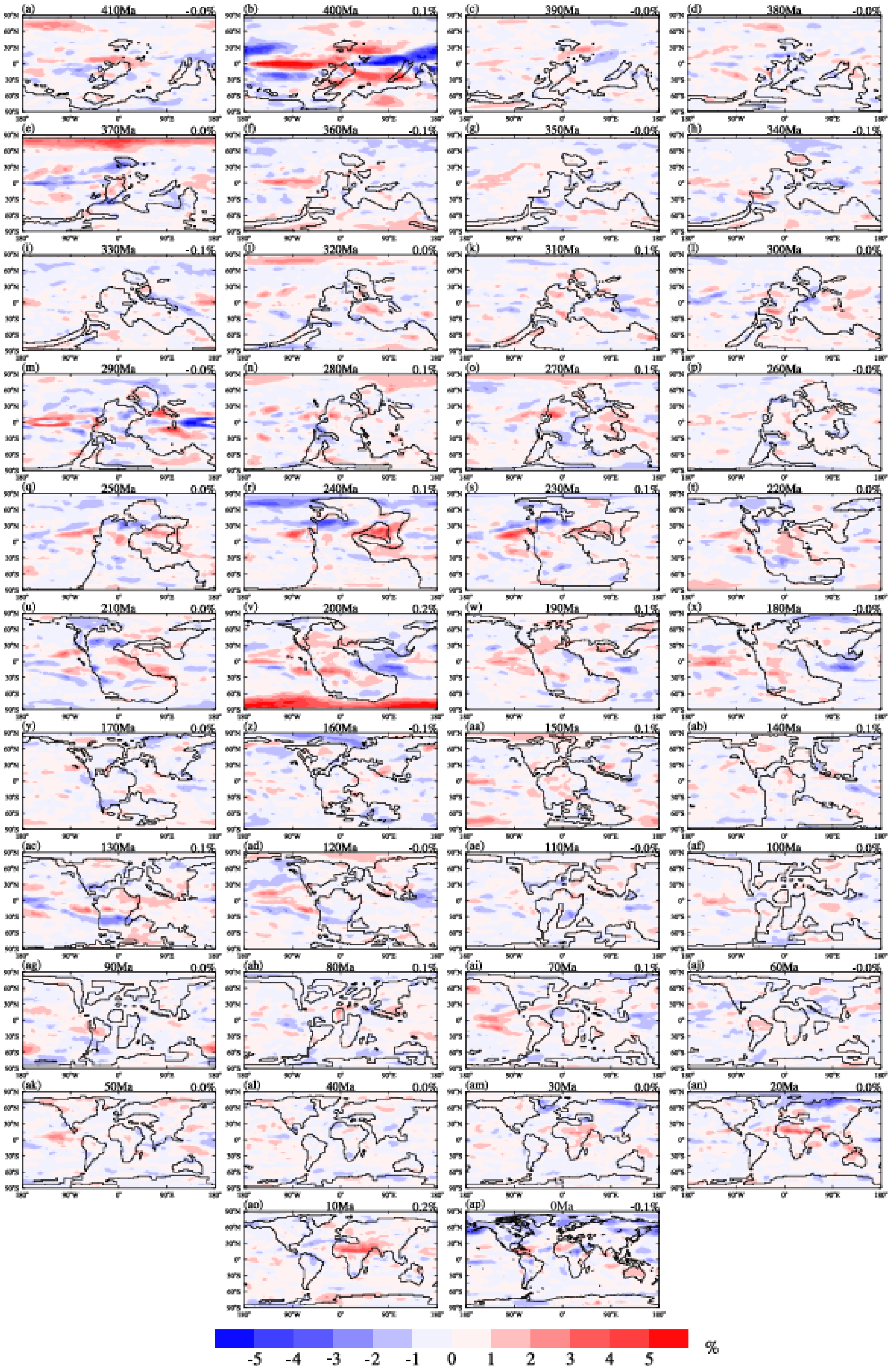

Figure S21. The differences of vertically-integrated total cloud fraction (%) between DUST2 experiments and DUST1 experiments for 410 Ma to 0 Ma.

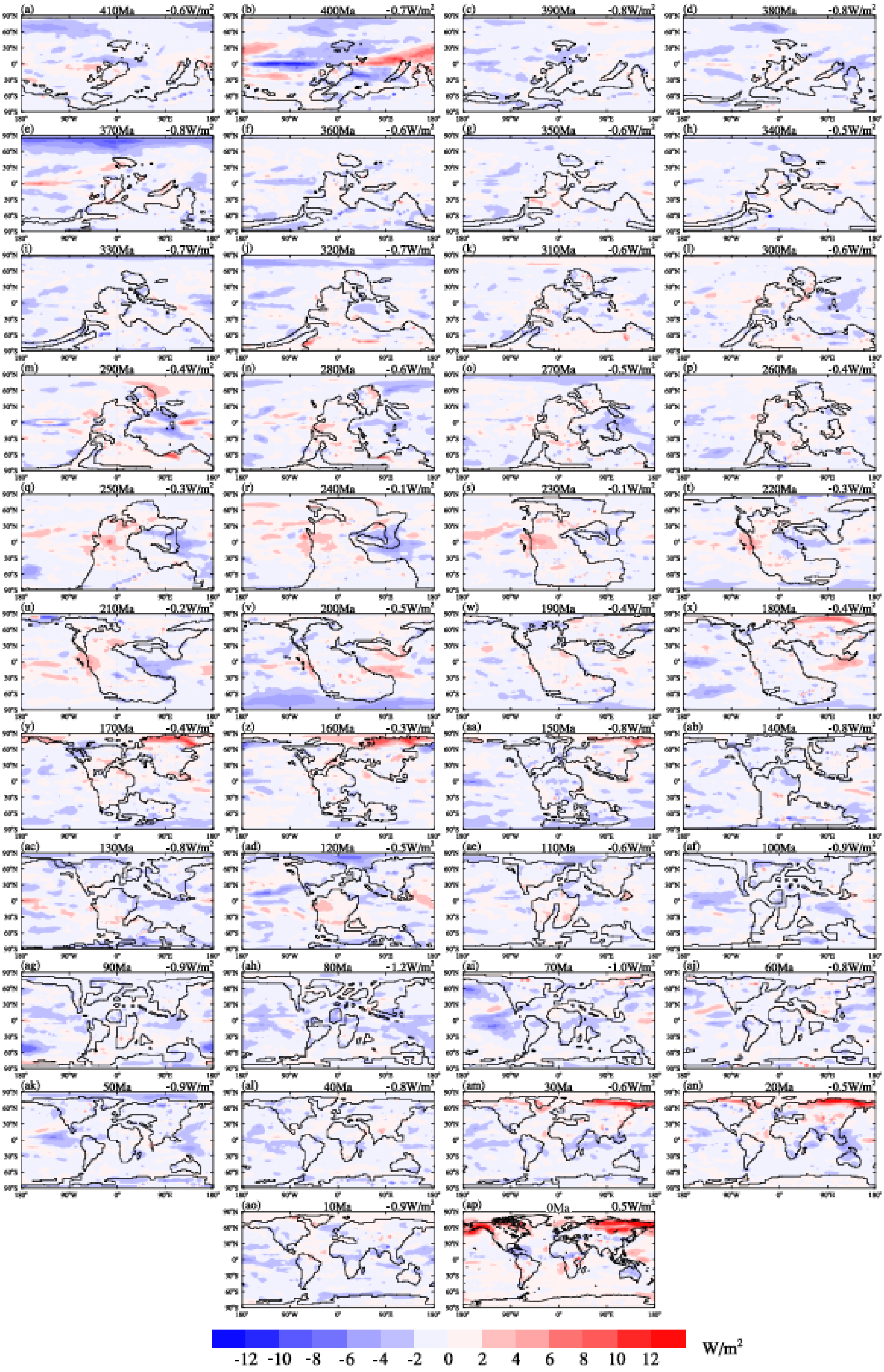

Figure S22. The differences of shortwave cloud forcing (W/m^2) between DUST2 experiments and DUST1 experiments for 410 Ma to 0 Ma.

Table S1. Atmospheric CO_2 concentrations, solar radiation, and simulated dust emission, dust loading, dust deposition into ocean, dust lifetime, global mean surface temperatures (GMSTs) for the 55 simulations (DUST2) in this study.

Simulation	Year (Ma)	CO_2 (ppmv)	Solar radiation (W/m^2)	Dust				GMST (°C)
				Emission (Tg/yr)	Loading (Tg)	Deposition into ocean (Tg/yr)	Lifetime (day)	
1	540	7840	1302.20	6228.2	53.2	2391.5	3.1	25.81
2	530	7560	1303.29	6595.2	56.9	2555.1	3.1	25.71
3	520	6440	1304.38	5841.9	47.0	2210.3	2.9	25.41
4	510	6440	1305.47	6643.8	49.0	2427.3	2.7	25.25
5	500	7000	1306.56	5833.1	44.7	2064.7	2.8	25.32
6	490	7000	1307.65	6801.3	49.9	2420.2	2.7	25.53
7	480	6720	1308.74	6718.6	44.6	2337.9	2.4	25.86
8	470	6440	1309.83	6769.1	47.3	2373.5	2.5	25.77
9	460	4480	1310.92	6748.6	46.4	2389.7	2.5	23.57
10	450	1680	1312.00	6179.6	42.4	2381.8	2.5	18.48
11	440	1680	1313.09	5839.3	42.3	2159.1	2.6	18.10
12	430	1960	1314.18	5454.7	37.1	2237.3	2.5	20.82
13	420	1680	1315.27	8220.4	52.2	3384.4	2.3	21.12
14	410	1260	1316.36	216.6	2.8	98.1	4.7	21.96
15	400	1400	1317.45	140.0	1.9	62.6	4.9	23.02
16	390	2660	1318.54	212.7	3.2	90.6	5.4	24.71
17	380	2800	1319.63	167.3	2.7	71.0	5.8	24.93
18	370	1680	1320.71	134.7	1.9	56.1	5.1	22.60
19	360	1260	1321.8	57.3	0.5	23.0	3.2	20.48
20	350	1120	1322.89	128.1	1.6	33.7	4.5	19.55
21	340	1260	1323.98	313.9	4.6	85.1	5.3	20.20
22	330	980	1325.07	484.3	6.6	156.8	4.9	18.97
23	320	840	1326.16	723.3	9.8	200.2	4.9	16.64
24	310	532	1327.25	715.6	9.4	212.0	4.8	13.27
25	300	532	1328.34	767.0	10.5	247.5	5.0	16.05
26	290	420	1329.42	886.0	11.0	252.5	4.5	12.61
27	280	532	1330.51	997.5	14.0	269.6	5.1	15.11
28	270	896	1331.6	969.5	14.6	278.5	5.5	19.27
29	260	1680	1332.69	1079.1	16.4	329.1	5.5	22.40
30	250	4424	1333.78	1581.3	27.0	384.9	6.2	25.51
31	240	4760	1334.87	1981.3	35.0	496.7	6.4	25.28
32	230	4200	1335.96	1539.2	29.1	367.3	6.9	24.84
33	220	3640	1337.05	1023.6	18.9	274.0	6.7	24.42
34	210	3360	1338.14	1017.5	18.6	252.5	6.6	23.89
35	200	2800	1339.22	1152.6	19.8	263.7	6.2	22.66
36	190	1680	1340.31	897.5	14.2	226.0	5.7	20.43
37	180	1484	1341.4	706.4	10.6	155.3	5.5	19.38
38	170	1120	1342.49	913.2	12.0	257.6	4.8	18.77
39	160	980	1343.58	1119.7	13.6	385.1	4.4	19.19
40	150	1120	1344.67	521.0	6.3	146.5	4.4	19.76

41	140	1358	1345.76	637.7	8.9	186.1	4.6	20.31
42	130	1288	1346.85	600.1	9.6	153.8	5.8	21.47
43	120	1400	1347.93	582.9	8.9	160.7	5.5	22.57
44	110	1400	1349.02	299.2	3.7	111.8	4.5	23.34
45	100	1540	1350.11	202.8	2.8	79.4	5.0	23.78
46	90	1260	1351.2	256.1	3.2	102.3	4.5	23.58
47	80	1211	1352.29	230.4	3.0	94.9	4.7	24.21
48	70	1260	1353.38	79.5	1.1	32.3	5.0	23.06
49	60	980	1354.47	174.7	2.2	46.8	4.6	21.98
50	50	1064	1355.56	237.9	3.2	57.4	4.9	22.77
51	40	728	1356.64	313.1	4.2	67.9	4.9	20.56
52	30	504	1357.73	926.9	13.9	210.2	5.5	16.28
53	20	504	1358.82	1148.3	17.6	288.9	5.6	15.59
54	10	476	1359.91	797.2	12.2	178.5	5.6	16.16
55	0	280	1360.89	2217.8	23.4	991.3	3.8	12.03

Table S2. Compilation of main aeolian sand systems used in this study. This compilation is modified and expanded from Rodríguez-López et al. (2014).

Period	simulation	Location	Basin	Key reference
Early Devonian	410Ma, 400Ma, 390Ma	Scotland	Orcadian Basin Extensional basin	Marshall et al. (1996)
		Scotland	Orcadian Basin	Rogers & Astin (1991)
		Scotland	Shetland basin	Allen & Marshall (1981)
		Scotland	Fault bounded basins	Trewin & Thirlwall (2002)
		Australia	Canning Basin	Thornton (1990)
		Antarctica		Gilmer (2008)
		Saudi Arabia		Stump & Vandereem (1995)
		Ireland	Intracontinental rift setting	Morrissey et al. (2012)
Early Carboniferous	360Ma, 350Ma, 340Ma, 330Ma	USA	Appalachian Basin	Swezey et al. (2012)
		Saudi Arabia		Stump & Vandereem (1995)
		Greenland	Intramontane strike-slip basin	Olsen & Larsen (1993)
Late Carboniferous	320Ma, 310Ma, 300Ma, 290Ma	Canada		Stewart & Walker (1980)
		USA	Green River basin	Driese & Dott (1984)
		USA	Eagle Basin	Schenk 1987
		USA	Paradox foreland basin	Jordan & Mountney (2012)
		USA	Michigan Basin	Benison et al. (2011)
		USA	Uinta–Piceance	Bowker & Jackson

			Badin Province	(1989)
		USA		Chan & Kocurek (1988)
		USA	Laramie Basin	Kelly (1984)
		USA		Kerr & Dott (1988)
		USA		Loope & Haverland (1988)
		Brazil	Solimões Basin	Elias et al. (2007)
		Argentina	Paganzo basin	Geuna et al. (2010)
		Argentina	Tarija Basin	Hernández & Echavarria (2009)
Late Permian	260Ma, 250Ma	Argentina	Paganzo Basin retroarc basin	Spalletti et al. (2010); Limarino & Spalletti (1986)
		Argentina	Mendoza Province	Limarino & Spalletti (1986)
		Argentina	Northern Precordillera	Limarino & Spalletti (1986)
		Argentina	La Rioja Province	Limarino & Spalletti (1986)
		Brazil	Paraná Basin	Giannini et al. (2004) Dias & Scherer (2008)
		USA		Edwin (1979)
		Scotland	Arran Basin Pull-apart basin	Clemmensen & Abrahamsen (1983)
		UK	Moray Firth Basin Northern North Sea Basin	Clemmensen (1987) Hurst & Glennie (2008)
		UK	Dorset Basin	Newell (2001)
		UK	Worcester Basin and Shropshire Basin	Benton et al. (2002)
		Poland	Polish Rotliegend Basin	Kiersnowski & Buniak (2006)
		Germany	North German Basin; Southern Permian Basin	Antrett et al. (2012)
		Denmark	Northern Permian Basin	Heward Alan et al. (2003)
		Netherlands	Southern Permian Basin	Geluck (2007)
		France	Champenay Basin	Swezey et al. (1996)
		Norway	Rendalen Graben, Oslo Rift	Larsen et al. (2008)
Early Triassic	240Ma, 230Ma	Germany	Central European Basin	Bourquin et al. (2009)
		France	Rift basin	Maubeuge (1974)

		Spain	Iberian Basin	Soria et al. (2011)
		Heliogoland		Clemmensen & Hegner (1991)
		Poland		Mroczkowski & Mader (1985)
		Scotland		Hurst & Glennie (2008)
		Scotland		Tyrrell et al. (2009)
		Ireland	East Irish Sea Basin	Buckman et al. (1998)
		England		Cowan & Boycott-Brown (2003) Meadows (2006)
		England	West Cumbrian Basin	Jones & Ambrose (1994)
		England	Cheshire Basin	Bloomfield et al. (2006)
		USA		Irmen & Vondra (2000)
		USA	Paradox Basin	Lawton & Buck (2006)
		Canada	Extensional basin; Peace River Basin	Davies et al. (1997) Nassichuk (2000)
		Southern Africa	Karoo Basin	Edwin (1979)
		India	Auranga–Gondwana Basin	Sen & Sinha (1985)
Early Jurassic	200Ma, 190Ma, 180Ma	Brazil	Paraná Basin	Nowatzki & Kern (2000)
		Argentina		Silva & Fernandez (2004)
		USA	Back-arc basin	Tanner & Lucas (2007); Porter (1987)
		USA	Retro-foreland basin; flexural basin and back-arc basin	Edwards (1985) Tanner & Lucas (2007)
		USA	San Juan Basin	Huffman et al. (1984)
		USA		Aultman (1975)
		USA	Michigan Basin; intracratonic basin	Benison et al. (2011)
		USA	Pomperaug Basins	LeTourneau & Huber (2006)
		Canada	Fundy Basin	Tanner & Hubert (1992)
		South Africa	Tuli Basin	Holzförster (2007)
		Morocco	Argana Basin	Hofmann et al. (2000)
Late Jurassic	170Ma, 160Ma, 150Ma	Brazil	Paraná Basin	Nowatzki & Kern (2000); Scherer & Lavina (2006)
		Brazil	Parnaiba Basin	Edwin (1979)

		Brazil	Recôncavo Basin	Bongiolo & Scherer (2010)
		Argentina	Neuquén Basin; backarc basin	Veiga & Spalletti (2007)
		Chile	North–south-elongated intermontane back-arc basin	Bell (1991)
		USA		Allen et al. (2000); Anderson & Lucas, (1984)
		USA	Uinta Basin	Keele (2008)
		USA		Lockley et al. (2007)
		USA		O'Sullivan (2010)
		USA	Chama Basin	Lucas et al. (2005)
		USA	San Juan Basin	Huffman et al. (1984)
		USA	Bighorn Basin	Kilibarda & Loope (1997)
		USA, Mexico	Gulf of Mexico	Ajdukiewicz et al. (2010)
		USA, Mexico		Tedesco et al. (2002)
		USA		Aultman (1975)
		USA	Michigan Basin; intracratonic basin	Benison et al. (2011)
		USA		Szigeti & Fox (1981)
		Mexico	Central Coahuila	González-Naranjo et al. (2008)
Early Cretaceous	140Ma, 130Ma, 120Ma, 110Ma	Brazil	Parnaiba Basin.	Edwin (1979)
		Brazil	Paraná Basin	Edwin (1979)
		Brazil	Recôncavo Basin	Bongiolo & Scherer (2010)
		Brazil	Sanfranciscana Basin	Mendonca & Castro (2002)
		Chile	North–south-elongated intermontane back-arc basin	Bell (1991)
		Argentina	Neuquén Basin	Strömbäck et al. (2005)
		Central and Southern Africa	Kalahari and Okavango basins; intracratonic sag basins	Haddon & McCarthy (2005)
		Namibia	Huab Basin	Howell & Mountney (2001)
		Namibia		Mello et al. (2011)
		Namibia		Goudie & Eckardt

				(1999)
		Egypt		Ahmed & Soliman (1988)
		Israel	Maktesh Gadol	Azmon (1982)
		Israel		Weinberger (1980)
		Mongolia, China	Gobi Desert	Jerzykiewicz et al. (1989)
		Tibet	Nima Basin	DeCelles et al. (2007)
		China		Chen et al. (1994) Jiang et al. (2008) Li et al. (2004) Mei et al. (2003)
		Thailand	Khorat Basin	Hasegawa et al. (2009)
		France	Saleve Chain	Kindler & Davaud (2001)
		Greece		Mizota et al. (1988)
		North Atlantic	North Atlantic Ocean Basin	Lever & McCave (1983)
		Mexico	Central Coahuila	González-Naranjo et al. (2008)
Late Cretaceous	100Ma, 90Ma, 80Ma, 70Ma	Brazil	Bauru Basin; intracratonic basin	Basilici & Fuhr-Dal (2010)
		Brazil		Sgarbi & Ladeira (1995)
		Brazil	Sanfranciscana Basin	Spigolon & Alvarenga (2002)
		Argentina	Central Argentinean rift	Rivarola & Spalletti (2006)
		Argentina	Neuquén Basin	Sánchez & Heredia (2006)
		Argentina	Neuquén Basin	Sánchez et al.(2006)
		Argentina	Neuquén Basin	Armas et al. (2012)
		Mongolia	Ulan Nur Basin	Seike et al. (2010)
		China	Bayan Mandahu	Eberth (1993)
		Mongolia, China	Gobi Desert	Jerzykiewicz et al. (1989)
		Tibet	Nima Basin	DeCelles et al. (2007)
		China	.	Chen et al. (1994) Jiang et al. (2008) Li et al. (2004) Mei et al. (2003)
		Thailand	Khorat Basin	Hasegawa et al. (2009)
		Greece		Mizota et al. (1988)
		North Atlantic	North Atlantic Ocean Basin	Lever & McCave (1983)
		Mid-Pacific Mountains	Pacific Ocean Basin	Rea & Janecek (1981)

		USA	Kaiparowits Basin	Simpson et al. (2008)
Middle Eocene	50Ma, 40Ma	France	Paris Basin	Thiry et al. (1988)
		USA	Uplifted Colorado Plateau	Cather et al. (2008)
		USA	Great Plains	Tedford et al. (1996)
		Gabon	Congo Basin	Seranne et al. (2008)
		Egypt	Fayum Basin	El-Fawal et al. (2013)
		Morocco	Tindoouf-Ouarzazate Basin	Tesón et al. (2010)
		Australia	Eucla Basin	Hou et al. (2006)
		China	Xining Basin	Meijer et al. (2021)
		China	Xorkol Basin	Li et al. (2018)
		China	Lanzhou Basin	Zhang et al. (2014)
Miocene	20Ma-10Ma	Portugal	Lower Tejo Basin	Pais et al. (2012)
		Italy	Valdarno Basin	Ghinassi et al. (2004)
		Spain	Teruel Basin	Rodríguez-López et al. (2012)
		USA	Río Grande Rift, Albuquerque basin	Galusha & Blick (1971)
		USA	Aggrading High Plains of USA	Bart (1977)
		USA	La Española Basin	Koning et al. (2004)
		USA	Extensional Knoll Basin.	Deibert & Camilleri (2006)
		Mexico	Forearc Basin	Umhoefer et al. (2001)
		Bolivia	Andean Foreland	Uba et al. (2005)
		Argentina	Andean Foreland	Voss (2002)
		Argentina	Andean Foreland	Tripaldi & Limarino (2005)
		Argentina	Active Andean foreland	Milana et al. (1993)
		Argentina	Andean Foreland	Do Campo et al. (2010)
		Argentina	Andean (Broken) Foreland	Dávila & Astini (2003)
		Argentina	Andean Foreland	Irigoyen et al. (2000)
		Argentina	Northern Magallanes Basin/San Jorge Basin	Bown & Larriestra (1990)
		Argentina	.	Zavala & Freije (2001)
		Saudi Arabia		Bristow (1999)
		Namibia		Segalen et al. (2004)
		Chad	Intracratonic Chad Basin	Swezey (2006)
		Western Cape		Franceschini & Compton (2004)

		China	Lanzhou Basin	Zhang et al. (2014)
		China	Sikouzi area	Jiang & Ding (2010)
		China	Central Loess Plateau	Ding et al. (2001); Sun et al. (1997)
		China	Baode	Zhu et al. (2008)
		China	Jiaxian	Ding et al. (1998); Qiang et al. (2001)
		China	Shilou	Xu et al. (2009)

References

Ahmed, E. A. & M. A. Soliman. Quartz surface textures of some Cretaceous Nubian sandstone exposures. J. Afr. Earth Sci 7, 873–878 (1988).

Ajdukiewicz, J. M., P. H. Nicholson & W. L. Esch. Prediction of deep reservoir quality using early diagenetic process models in the Jurassic Norphlet Formation, Gulf of Mexico. AAPG BULLETIN 94(8), 1189-1227 (2010). https://doi.org/10.1306/04211009152

Allen, P. A. & J. E. A. Marshall. DEPOSITIONAL-ENVIRONMENTS AND PALYNOLOGY OF THE DEVONIAN SOUTHEAST SHETLAND BASIN. SCOTTISH JOURNAL OF GEOLOGY 17, 257-273 (1981). https://doi.org/10.1144/sjg17040257

Allen, P. A., J. E. Verlander, P. M. Burgess & D. M. Audet. Jurassic giant erg deposits, flexure of the United States continental interior and timing of the onset of Cordilleran shortening. Geology 28, 159–162 (2000).

Antrett, P., A. A. Vackiner, P. A. Kukla, S. Back & H. Stollhofen. Controls on reservoir compartmentalization of an Uper Permian tight gas field in Germany and links to a modern analogue in the Western US. Petrol. Geosci 18, 289–304 (2012).

Armas, P., C. Moreno & M. L. Sánchez. Areniscas eólicas y mareales del Cretácico Superior de la Cuenca Neuquina (Argentina). Análisis petrográfico y de procedencia. Rev. Soc. Geol. Esp 25, 193–207 (2012).

Aultman, W. L. The subsurface Jurassic Bay Springs Sand. Transactions - Gulf Coast Ass. Geol. Socs 25, 217–229 (1975).

Azmon, E. Ventispheres: granule-pebble spheres of eolian origin in Lower Cretaceous and Recent rocks of Israel. Sed. Geol 33, 57–71 (1982).

Bart, H. A. SEDIMENTOLOGY OF CROSS-STRATIFIED SANDSTONES IN ARIKAREE GROUP, MIOCENE, SOUTHEASTERN WYOMING. SEDIMENTARY GEOLOGY 19(3), 165-184 (1977). https://doi.org/10.1016/0037-0738(77)90029-X

Basilici, G. & B. P. F. Fuhr-Dal. Anatomy and controlling factors of a Late Cretaceous aeolian sand sheet: The Marilia and the Adamantina formations. NW Bauru Basin, Brazil. Sed. Geol 226, 71–93 (2010).

Bell, C. M. The relationships between sedimentary structures, transport directions and dune types in Mesozoic aeolian sandstones, Atacama Region, Chile. Sedimentology 38, 289–300 (1991).

Benison, K. C., J. P. Knapp & J. M. Dannenhoffer. The Pennsylvanian Pewamo Formation and associated Haybridge strata; toward the resolution of the Jurassic Ionia red bed problem in the Michigan Basin. U. S. A. J. Sed. Res 81, 459–478 (2011).

Benton, M. J., E. Cook & P. Turner. Permian and Triassic Red Beds and the Penarth Group of Great Britain, JNCC (2002).

Bloomfield, J. P., M. F. Moreau & A. J. Newell. Characterization of permeability distributions in six lithofacies from the Helsby and Wilmslow sandstone formations of the Cheshire Basin, UK. FLUID FLOW AND SOLUTE MOVEMENT IN SANDSTONES: THE ONSHORE UK PERMO-TRIASSIC RED BED SEQUENCE. 263: 83-+ (2006).

Bongiolo, D. E. & C. M. S. Scherer. Facies architecture and heterogeneity of the fluvial–aeolian reservoirs of the Sergi formation (Upper Jurassic), Recôncavo Basin, NE Brazil. Marine and Petroleum Geology 27(9), 1885-1897 (2010). https://doi.org/https://doi.org/10.1016/j.marpetgeo.2010.07.015

Bourquin, S., F. Guillocheau & S. PÉRon. Braided rivers within an arid alluvial plain (example from the Lower Triassic, western German Basin): recognition criteria and expression of stratigraphic cycles. Sedimentology 56(7), 2235-2264 (2009). https://doi.org/https://doi.org/10.1111/j.1365-3091.2009.01078.x

Bowker, K. A. & W. D. Jackson. The Weber Sandstone at Rangely field, Colorado.In E. B. Coalson. Petrogenesis and petrophysics of selected sandstone reservoirs of the Rocky Mountain region. Rocky Mountain Association of Geologists Annual Guidebook: 65–80 (1989).

Bown, T. M. & C. N. Larriestra. SEDIMENTARY PALEOENVIRONMENTS OF FOSSIL PLATYRRHINE LOCALITIES, MIOCENE PINTURAS FORMATION, SANTA-CRUZ-PROVINCE, ARGENTINA. JOURNAL OF HUMAN EVOLUTION 19(1-2), 87-119 (1990). https://doi.org/10.1016/0047-2484(90)90013-2

Bristow, C. S. Aeolian and sabkha sediments in the Miocene Shuwaihat Formation, Emirate of Abu Dhabi, United Arab Emirates.In E. P. J. Whybrow and A. Hill. Fossil Vertebrates of Arabia: 50–60. New Haven, Yale University Press (1999).

Buckman, J. O., P. S. Doughty, M. J. Benton & A. J. Jeram. Palaeoenvironmental interpretation of the Triassic sandstones of Scrabo, County Down, Northern Ireland; ichnological and sedimentological studies indicating a mixed fluviatile-aeolian succession. Irish J. Earth Sci 16, 85–102 (1998).

Cather, S. M., S. D. Connell, R. M. Chamberlin, W. C. McIntosh, G. E. Jones, A. R. Potochnik, et al. The Chuska erg: Paleogeomorphic and paleoclimatic implications of an Oligocene sand sea on the Colorado Plateau. GEOLOGICAL SOCIETY OF AMERICA BULLETIN 120(1-2), 13-33 (2008). https://doi.org/10.1130/B26081.1

Chan, M. A. & G. Kocurek. COMPLEXITIES IN EOLIAN AND MARINE INTERACTIONS - PROCESSES AND EUSTATIC CONTROLS ON ERG DEVELOPMENT. SEDIMENTARY GEOLOGY 56(1-4), 283-300 (1988). https://doi.org/10.1016/0037-0738(88)90057-7

Chen, R., H. Zhu, Y. Chen & L. Xu. Recognition of aeolian sandstone of Lower Cretaceous in the southwest depression of Tarim Basin and its significance. Chinese Sci. Bull 39, 754–758 (1994).

Clemmensen, L. B. & K. Abrahamsen. Aeolian stratification and facies association in desert sediments, Arran basin (Permian), Scotland. Sedimentology 30(3), 311-339 (1983). https://doi.org/https://doi.org/10.1111/j.1365-3091.1983.tb00676.x

Clemmensen, L. B. Complex star dunes and associated aeolian bedforms, Hopeman Sandstone (Permo-Triassic), Moray Firth Basin, Scotland. Geological Society, London, Special Publications 35(1), 213-231 (1987). https://doi.org/10.1144/GSL.SP.1987.035.01.15

Clemmensen, L. B. & J. Hegner. Eolian sequence and erg dynamics; the Permian Corrie Sandstone, Scotland. Journal of Sedimentary Research 61(5), 768-774 (1991). https://doi.org/10.1306/D42677CB-2B26-11D7-8648000102C1865D

Cowan, G. & T. Boycott-Brown. The North Morecambe Field, Block 110/2a, East Irish Sea. Geological Society, London, Memoirs 20(1), 97-105 (2003). https://doi.org/10.1144/GSL.MEM.2003.020.01.08

Davies, G. R., T. F. Moslow & M. D. Sherwin. The Lower Triassic Montney Formation, west-central Alberta. BULLETIN OF CANADIAN PETROLEUM GEOLOGY 45(4), 474-505 (1997).

Dávila, F. M. & R. A. Astini. The eolian beds of the Famatina range:: Middle miocene paleoclimate-tectonic interaction in the central Andean broken foreland? REVISTA GEOLOGICA DE CHILE 30(2), 187-204 (2003).

DeCelles, P. G., P. Kapp, L. Ding & G. E. Gehrels. Late Cretaceous to middle Tertiary basin evolution in the central Tibetan Plateau: Changing environments in response to tectonic partitioning, aridification, and regional elevation gain. GSA Bulletin 119(5-6), 654-680 (2007). https://doi.org/10.1130/B26074.1

Deibert, J. E. & P. A. Camilleri. Sedimentologic and tectonic origin of an incised-valley-fill sequence along an extensional marginal-lacustrine system in the Basin and Range province, United States: Implications for predictive models of the location of incised valleys. AAPG Bulletin 90(2), 209-235 (2006). https://doi.org/10.1306/09140505028

Dias, K. D. N. & C. M. S. Scherer. Cross-bedding set thickness and stratigraphic architecture of aeolian systems: An example from the Upper Permian Piramboia Formation (Parana' Basin), southern Brazil. JOURNAL OF SOUTH AMERICAN EARTH SCIENCES 25(3), 405-415 (2008). https://doi.org/10.1016/j.jsames.2007.07.008

Do Campo, M., C. del Papa, F. Nieto, F. Hongn & I. Petrinovic. Integrated analysis for constraining palaeoclimatic and volcanic influences on clay-mineral assemblages in orogenic basins (Palaeogene Andean foreland, Northwestern Argentina). SEDIMENTARY GEOLOGY 228(3-4), 98-112 (2010). https://doi.org/10.1016/j.sedgeo.2010.04.002

Driese, S. G. & R. H. Dott, Jr. Model for Sandstone-Carbonate “Cyclothems” Based on Upper Member of Morgan Formation (Middle Pennsylvanian) of Northern Utah and Colorado. AAPG Bulletin 68(5), 574-597 (1984). https://doi.org/10.1306/AD461340-16F7-11D7-8645000102C1865D

Eberth, D. A. Depositional environments and facies transitions of dinosaur-bearing Upper Cretaceous redbeds at Bayan Mandahu (Inner Mongolia, People's Republic of China). Canadian Journal of Earth Sciences 30(10), 2196-2213 (1993). https://doi.org/10.1139/e93-191

Edwin, M. A study of global sand seas. Professional Paper. Washington, D.C.: 439 (1979).

El-Fawal, F. M., H. M. El-Asmar & M. A. E.-F. Sarhan. Depositional evolution of the Middle-Upper Eocene rocks, Fayum area, Egypt. Arabian Journal of Geosciences 6(3), 749-760 (2013). https://doi.org/10.1007/s12517-011-0386-4

Elias, A. D., L. F. De Ros, A. M. Mizusaki & K. Kawashita. Isotopic evidence on the diagenetic evolution of coastal sabkha reservoirs from the Solimoes Basin, northern Brazil. GONDWANA RESEARCH 11(4), 553-567 (2007). https://doi.org/10.1016/j.gr.2006.06.007

Franceschini, G. & J. S. Compton. Aeolian and marine deposits of the Tabakbaai Quarry area, western Cape, South Africa. SOUTH AFRICAN JOURNAL OF GEOLOGY 107(4), 619-632 (2004). https://doi.org/10.2113/107.4.619

Geluck, M. C. Permian.In D. A. J. B. Eds Th.E. Wong and J. Jager. Geology of the Netherlands: 63–83 (2007).

Geuna, S. E., L. D. Escosteguy & C. O. Limarino. Paleomagnetism of the Carboniferous-Permian Patquia Formation, Paganzo basin, Argentina: implications for the apparent polar wander path for South America and Gondwana during the Late Palaeozoic. GEOLOGICA ACTA 8(4), 373-397 (2010). https://doi.org/10.1344/105.000001578

Ghinassi, M., M. Magi, M. Sagri & B. S. Singer. Arid climate 2.5 Ma in the Plio-Pleistocene Valdarno Basin (Northern Apennines, Italy). PALAEOGEOGRAPHY PALAEOCLIMATOLOGY PALAEOECOLOGY 207(1-2), 37-57 (2004). https://doi.org/10.1016/j.palaeo.2004.01.020

Giannini, P. C. F., A. O. Sawakuchi, A. L. Fernandes & L. M. Donatti. Paleoventos e paleocorrentes subaquosas do sistema deposicional Pirambóia nos estados de São Paulo e Paraná, Bacia do Paraná: estudo baseado em análise estatística de dados azimutais. Revista Brasileira de Geociências 34(2), 282-292 (2004). https://doi.org/10.25249/0375-7536.2004342282292

Gilmer, G. (2008). Paleoenvironmental Interpretations of the Lower Taylor Group, Olympus Range area, southern Victoria Land, Antarctica.

González-Naranjo, G. A., R. S. Molina-Garza & G. Chávez-Cabello. Paleomagnetic study of Jurassic and Cretaceous rocks north of San Marcos Fault, central Coahuila, Mexico. Geofísica Internacional 47, 41–55 (2008).

Goudie, A. S. & F. Eckardt. The evolution of the morphological framework of the Central Namib Desert, Namibia, since the Early Cretaceous. GEOGRAFISKA ANNALER SERIES A-PHYSICAL GEOGRAPHY 81A(3), 443-458 (1999).

Haddon, I. G. & T. S. McCarthy. The Mesozoic-Cenozoic interior sag basins of Central Africa: The Late-Cretaceous-Cenozoic Kalahari and Okavango basins. JOURNAL OF AFRICAN EARTH SCIENCES 43(1-3), 316-333 (2005). https://doi.org/10.1016/j.jafrearsci.2005.07.008

Hasegawa, H., R. Tada, N. Ichinnorov & C. Minjin. Lithostratigraphy and depositional environments of the Upper Cretaceous Djadokhta Formation, Ulan Nuur basin, southern Mongolia, and its paleoclimatic implication. J. Asian Earth Sci 35, 13–26 (2009).

Hernández, R. & L. Echavarria. Subandean fold and thrust belt of Northwest Argentina: stratigraphy, geometry, and chronology of deformation. Revista de la Asociación Geológica Argentina 65(1), 068-080 (2009).

Heward Alan, P., P. Schofield & G. Gluyas Jon. The Rotliegend reservoir in Block 30/24, UK Central North Sea: including the Argyll (renamed Ardmore) and Innes fields. Petroleum Geoscience 9(4), 295-307 (2003). https://doi.org/10.1144/1354-079303-578

Hofmann, A., A. Tourani & R. Gaupp. Cyclicity of Triassic to Lower Jurassic continental red beds of the Argana Valley, Morocco: implications for palaeoclimate and basin evolution. Palaeogeography, Palaeoclimatology, Palaeoecology 161(1), 229-266 (2000). https://doi.org/https://doi.org/10.1016/S0031-0182(00)00125-5

Holzförster, F. Lithology and depositional environments of the Lower Jurassic Clarens Formation in the eastern Cape, South Africa. SOUTH AFRICAN JOURNAL OF GEOLOGY 110(4), 543-560 (2007). https://doi.org/10.2113/gssajg.110.4.543

Hou, B., N. F. Alley, L. A. Frakes, L. Stoian & W. M. Cowley. Eocene stratigraphic succession in the Eucla Basin of South Australia and correlation to major regional sea-level events. SEDIMENTARY GEOLOGY 183(3-4), 297-319 (2006). https://doi.org/10.1016/j.sedgeo.2005.10.007

Howell, J. & N. Mountney. Aeolian grain flow architecture: hard data for reservoir models and implications for red bed sequence stratigraphy. PETROLEUM GEOSCIENCE 7(1), 51-56 (2001). https://doi.org/10.1144/petgeo.7.1.51

Hurst, A. & K. W. Glennie. Mass-wasting of ancient aeolian dunes and sand fluidization during a period of global warming and inferred brief high precipitation: the Hopeman Sandstone (late Permian), Scotland. TERRA NOVA 20(4), 274-279 (2008). https://doi.org/10.1111/j.1365-3121.2008.00817.x

Irigoyen, M. V., K. L. Buchan & R. L. Brown. Magnetostratigraphy of Neogene Andean foreland-basin strata, lat 33°S, Mendoza Province, Argentina. GEOLOGICAL SOCIETY OF AMERICA BULLETIN 112(6), 803-816 (2000). https://doi.org/10.1130/0016-7606(2000)112<803:MONAFS>2.0.CO;2

Irmen, A. P. & C. F. Vondra. Aeolian sediments in lower to middle (?) Triassic rocks of central Wyoming. SEDIMENTARY GEOLOGY 132(1-2), 69-88 (2000). https://doi.org/10.1016/S0037-0738(99)00129-3

Jiang, H. & Z. Ding. Eolian grain-size signature of the Sikouzi lacustrine sediments (Chinese Loess Plateau): Implications for Neogene evolution of the East Asian winter monsoon. GSA Bulletin 122(5-6), 843-854 (2010). https://doi.org/10.1130/B26583.1

Jiang, X. S., Z. X. Pan, J. S. Xu, X. Y. Li, G. G. Xie & Z. J. Xiao. Late Cretaceous aeolian dunes and reconstruction of palaeo-wind belts of the Xinjiang Basin, Jiangxi Province, China. PALAEOGEOGRAPHY PALAEOCLIMATOLOGY PALAEOECOLOGY 257(1-2), 58-66 (2008). https://doi.org/10.1016/j.palaeo.2007.09.012

Jones, N. S. & K. Ambrose. Triassic sandy braidplain and aeolian sedimentation in the Sherwood Sandstone Group of the Sellafield area, west Cumbria. Proceedings of the Yorkshire Geological Society 50(1), 61-76 (1994). https://doi.org/10.1144/pygs.50.1.61

Jordan, O. D. & N. P. Mountney. SEQUENCE STRATIGRAPHIC EVOLUTION AND CYCLICITY OF AN ANCIENT COASTAL DESERT SYSTEM: THE PENNSYLVANIAN-PERMIAN LOWER CUTLER BEDS, PARADOX BASIN, UTAH, USA. JOURNAL OF SEDIMENTARY RESEARCH 82(9-10), 755-780 (2012). https://doi.org/10.2110/jsr.2012.54

Keele, D. J. (2008). The marriage of eolian rock properties and the style of structural deformation of the Nugget Formation; Anschutz Ranch East field: Northeast Utah and southwest Wyoming.

Kerr, D. R. & R. H. Dott. Eolian dune types preserved in the Tensleep Sandstone (Pennsylvanian-Permian), north-central Wyoming. Sedimentary Geology 56(1), 383-402 (1988). https://doi.org/https://doi.org/10.1016/0037-0738(88)90062-0

Kiersnowski, H. & A. Buniak. Evolution of the Rotliegend Basin of northwestern Poland. Geological Quarterly 50, 119-138 (2006).

Kindler, P. & E. Davaud. Recognizing eolianites in thin section, review and case study; the Lower Cretaceous Chambotte Formation, Saleve Chain, southeastern France. SEPM Special Publication 71, 141–150 (2001).

Koning, D. J., B. A. Scott & N. Dunbar. Middle-Upper Miocene stratigraphy of the Velarde Graben, north-central New Mexico: tectonic and paleogeographic implications. New Mexico Geological Society Guidebook, 55th Field Conference, Geology of the Taos Region: 359–373 (2004).

Larsen, B. T., S. Olaussen, B. Sunroll & M. Heeremans. The Permo-Carboniferous Oslo Rift through six stages and 65 million years. Episodes 31, 52–58 (2008).

Lawton, T. F. & B. J. Buck. Implications of diapir-derived detritus and gypsic paleosols in Lower Triassic strata near the Castle Valley salt wall, Paradox Basin, Utah. GEOLOGY 34(10), 885-888 (2006). https://doi.org/10.1130/G22574.1

LeTourneau, P. M. & P. Huber. Early Jurassic eolian dune field, Pomperaug basin, Connecticut and related synrift deposits: Stratigraphic framework and paleoclimatic context. Sed. Geol 187, 63–81 (2006).

Lever, A. & I. N. McCave. Eolian components in Cretaceous and Tertiary North Atlantic sediments. J. Sed. Petrol 53, 811–832 (1983).

Li, J. X., L. P. Yue, A. P. Roberts, A. M. Hirt, F. Pan, L. Guo, et al. Global cooling and enhanced Eocene Asian mid-latitude interior aridity. Nature Communications 9(1), 3026 (2018). https://doi.org/10.1038/s41467-018-05415-x

Li, X., Y. Hu, J. Guo, J. Lan, Q. Lin, X. Bao, et al. A high-resolution climate simulation dataset for the past 540 million years. Scientific Data (2022).

Li, Z., C. S, J. L, L. J & G. X. Interdune sedimentary genetic types and aeolian vertical sequence: An example from early Cretaceous continental paleodesert of Ordos. Di zhi ke ji qing bao 23, 30–34 (2004).

Limarino, C. P. & L. A. Spalletti. Eolian Permian deposits in west and northwest Argentina. Sed. Geol 49, 109–127 (1986).

Lockley, M., L. Mitchell & G. P. Odier. Small theropod track assemblages from Middle Jurassic eolianites of Eastern Utah: Paleoecological insights from dune ichnofacies in a transgressive sequence. Ichnos 14, 131–142 (2007).

Loope, D. B. & Z. E. Haverland. Giant desiccation fissures filled with calcareous eolian sand, Hermosa Formation (Pennsylvanian), southeastern Utah. Sed. Geol 56, 403–413 (1988).

Lucas, S. G., A. P. Hunt & J. A. Spielmann. Jurassic stratigraphy in the Chama Basin, New Mexico. New Mexico Geological Society 56th Field Conference Guidebook, Geology of the Chama Basin: 182–192 (2005).

Marshall, J. E. A., D. A. Rogers & M. J. Whiteley. Devonian marine incursions into the Orcadian Basin, Scotland. JOURNAL OF THE GEOLOGICAL SOCIETY 153, 451-466 (1996). https://doi.org/10.1144/gsjgs.153.3.0451

Maubeuge, P. L. Remarques sur les galets éolisés des grès du Trias lorrain (Remarks on eolian gravel of the Triassic sandstones of Lorrain, France. Bulletin de l'Académie et de la Société lorraine des Sciences 13, 21–22 (1974).

Meadows, N. S. The correlation and sequence architecture of the Ormskirk Sandstone Formation in the Triassic Sherwood Sandstone Group of the east Irish sea basin, NW England. GEOLOGICAL JOURNAL 41(1), 93-122 (2006). https://doi.org/10.1002/gj.1034

Mei, M., W. Jin, B. Yu, X. Lai, C. X & L. J. Study on sequence stratigraphy of the desert system, an example from the Lower Cretaceous in Kuche Basin, Xinjiang China. Xian dai di zhi 17, 59–67 (2003).

Meijer, N., G. Dupont-Nivet, N. Barbolini, A. Woutersen, A. Rohrmann, Y. Zhang, et al. Loess-Like Dust Appearance at 40 Ma in Central China. Paleoceanography and Paleoclimatology 36(3), e2020PA003993 (2021). https://doi.org/https://doi.org/10.1029/2020PA003993

Mello, M. R., N. Azambuja, W. U. Mohriak, A. J. Catto & J. B. Francolin. Promising giant new hydrocarbon frontier: the Namibian continental margin. GeoExpro 8, 64–69 (2011).

Mendonca, K. R. N. & J. C. Castro. Ciclicidade em depositos continentais da formacao Areado (Cretaceo inferior) na regiao de Galena-Varjao, sul da bacia Sanfranciscana (Cyclic sedimentation in terrestrial deposits of the Areado Formation (Lower Cretaceous), Galena-Varjao area, southern Sanfranciscana Basin.In Brasil. Boletim do 6o Simposio sobre o Cretaceo: 359–365 (2002).

Milana, J. P., M. Cevallos, A. Zavattieri, M. Pramparo & H. Papu. La secuencia terciaria de Pachaco: sedimentología, edad, correlaciones y significado paleogeográfico. XII Congreso Geológico Argentino. Actas 1, 226 234 (1993).

Mizota, C., M. Kusakabe & M. Noto. Eolian contribution to soil development on Cretaceous limestones in Greece as evidenced by oxygen isotope composition of quartz. Geochem. J 22, 41–46 (1988).

Morrissey, L. B., S. Braddy, C. Dodd, K. T. Higgs & B. P. J. Williams. Trace fossils and palaeoenvironments of the Middle Devonian Caherbla Group, Dingle Peninsula, southwest Ireland. GEOLOGICAL JOURNAL 47(1), 1-29 (2012). https://doi.org/10.1002/gj.1324

Mroczkowski, J. & D. Mader. Sandy inland braidplain deposition with local aeolian sedimentation in the lower and middle parts of the Buntsandstein and sandy coastal braidplain deposition in the topmost Zechstein in the Sudetes (Lower Silesia, Poland. Aspects of fluvial sedimentation in the Lower Triassic Buntsandstein of Europe 4, 165–195 (1985).

Nassichuk, B. R. Sedimentology, diagenesis and reservoir development of the Lower Triassic Montney Formation, northeastern British Columbia Masters Thesis, University of British Columbia (2000).

Newell, A. J. Bounding surfaces in a mixed aeolian-fluvial system (Rotliegend, Wessex Basin, SW UK. Mar. Petrol. Geol 18, 339–347 (2001).

Nowatzki, C. H. & H. P. Kern. The eolianites between Sanga do Cabral and Botucatu formations in Rio Grande do Sul state, Brazil. ANAIS DA ACADEMIA BRASILEIRA DE CIENCIAS 72(2), 247-256 (2000). https://doi.org/10.1590/S0001-37652000000200010

O'Sullivan, R. B. The lower and upper contacts of the Upper Jurassic Bluff Sandstone Member of the Morrison Formation in southeastern Utah. Geology of the Four Corners country 61, 101–106 (2010).

Olsen, H. & P. H. Larsen. Lithostratigraphy of the continental Devonian sediments, North-East Greenland. Geological Survey of Denmark and Greenland 165, 1-108 (1993). https://doi.org/10.34194/bullggu.v165.6721

Pais, J., P. P. Cunha, D. Pereira, P. Legoinha, R. Dias, D. Moura, et al. The Paleogene and Neogene of Western Iberia (Portugal), A Cenozoic record in the European Atlantic domain, Springer Briefs in Earth Sciences (2012).

Porter, M. L. Sedimentology of an ancient erg margin: The Lower Jurassic Aztec Sandstone, southern Nevada and southern California. Sedimentology 34, 661–680 (1987).

Qiang, X. K., Z. X. Li, C. M. Powell & H. B. Zheng. Magnetostratigraphic record of the Late Miocene onset of the East Asian monsoon, and Pliocene uplift of northern Tibet. Earth and Planetary Science Letters 187(1), 83-93 (2001). https://doi.org/https://doi.org/10.1016/S0012-821X(01)00281-3

Rea, D. K. & T. R. Janecek. Late Cretaceous history of eolian deposition in the mid-Pacific mountains, central North Pacific Ocean. Palaeogeogr. Palaeoclimatol. Palaeoecol 36, 55–67 (1981).

Rivarola, D. & L. A. Spalletti (2006). Model of continental sedimentation for the Cretaceous Central Argentinean rift: example from Las Quijadas hill, San Luis province.

Rodríguez-López, J. P., C. L. Liesa, J. Van Dam, P. Lafuente, L. Arlegui, L. Ezquerro & P. L. De Boer. Aeolian construction and alluvial dismantling of a fault-bounded intracontinental aeolian dune field (Teruel Basin, Spain); a continental perspective on Late Pliocene climate change and variability. SEDIMENTOLOGY 59(5), 1536-1567 (2012). https://doi.org/10.1111/j.1365-3091.2011.01316.x

Rodríguez-López, J. P., L. B. Clemmensen, N. Lancaster, N. P. Mountney & G. D. Veiga. Archean to Recent aeolian sand systems and their sedimentary record: Current understanding and future prospects. SEDIMENTOLOGY 61(6), 1487-1534 (2014). https://doi.org/10.1111/sed.12123

Rogers, D. A. & T. R. Astin. Ephemeral Lakes, Mud Pellet Dunes and Wind-Blown Sand and Silt: Reinterpretations of Devonian Lacustrine Cycles in North Scotland.In. Lacustrine Facies Analysis: 197-221 (1991).

Scherer, C. M. S. & E. L. C. Lavina. Stratigraphic evolution of a fluvial-eolian succession: The example of the Upper Jurassic-Lower Cretaceous Guara and Botucatu formations, Parana Basin, Southernmost Brazil. GONDWANA RESEARCH 9(4), 475-484 (2006). https://doi.org/10.1016/j.gr.2005.12.002

Segalen, L., P. Rognon, M. Pickford, B. Senut, L. Emmanuel, M. Renard & J. Ward. Reconstitution of dune morphologies and palaeowind regimes in the Proto-Namib since the Miocene. BULLETIN DE LA SOCIETE GEOLOGIQUE DE FRANCE 175(6), 537-546 (2004). https://doi.org/10.2113/175.6.537

Seike, K., H. Hasegawa & N. Ichinnorov. Preferred orientation of the trace fossil Entradichnus meniscus in eolian dune strata (Djadokhta Formation) at Tugrikiin Shiree, southern Mongolia and its paleoecological implications. ISLAND ARC 19(4), 622-627 (2010). https://doi.org/10.1111/j.1440-1738.2010.00742.x

Sen, D. P. & T. C. Sinha. TRIASSIC AEOLIAN SEDIMENTATION IN THE AURANGA-GONDWANA BASIN, BIHAR, INDIA. SEDIMENTARY GEOLOGY 43(1-4), 277-300 (1985). https://doi.org/10.1016/0037-0738(85)90060-0

Seranne, M., O. Bruguier & M. Moussavou. U-Pb single zircon grain dating of Present fluvial and Cenozoic aeolian sediments from Gabon: consequences on sediment provenance, reworking, and erosion processes on the equatorial West African margin. BULLETIN DE LA SOCIETE GEOLOGIQUE DE FRANCE 179(1), 29-40 (2008). https://doi.org/10.2113/gssgfbull.179.1.29

Simpson, E. L., H. L. Hilbert-Wolf, W. S. Simpson, S. E. Tindall, J. J. Bernard, T. A. Jenesky & M. C. Wizevich. The interaction of aeolian and fluvial processes during deposition of the Upper Cretaceous capping sandstone member, Wahweap Formation, Kaiparowits Basin, Utah, U.S.A. Palaeogeography, Palaeoclimatology, Palaeoecology 270(1), 19-28 (2008). https://doi.org/https://doi.org/10.1016/j.palaeo.2008.08.009

Soria, A. R., C. L. Liesa, J. P. Rodríguez-López, N. Meléndez, P. L. de Boer & A. Meléndez. An Early Triassic evolving erg system (Iberian Chain, NE Spain): palaeoclimate implications. TERRA NOVA 23(2), 76-84 (2011). https://doi.org/10.1111/j.1365-3121.2011.00986.x

Spalletti, L. A., C. O. Limarino & F. C. Piñol. Internal anatomy of an erg sequence from the aeolian-fluvial system of the De La Cuesta Formation (Paganzo Basin, northwestern Argentina). GEOLOGICA ACTA 8(4), 431-447 (2010). https://doi.org/10.1344/105.000001581

Spigolon, A. L. D. & C. J. S. Alvarenga. Facies e elementos arquiteturais resultantes de mudancas climaticas em um ambiente desertico; grupo Urucuia (Neocretaceo), Bacia Sanfranciscana, Brasil (Lithofacies and sedimentary structures derived from paleoclimatic changes in arid environments; Urucuia Group (Upper Cretaceous.In Brasil. Boletim do 6o Simposio sobre o Cretaceo: 367–373. Brazil, Sanfranciscana Basin (2002).

Stewart, W. D. & R. G. Walker. EOLIAN COASTAL DUNE DEPOSITS AND SURROUNDING MARINE SANDSTONES, ROCKY-MOUNTAIN SUPERGROUP (LOWER PENNSYLVANIAN), SOUTHEASTERN BRITISH-COLUMBIA. CANADIAN JOURNAL OF EARTH SCIENCES 17(9), 1125-1140 (1980). https://doi.org/10.1139/e80-120

Strömbäck, A., J. A. Howell & G. D. Veiga. The transgression of an erg - sedimentation and reworking/soft-sediment deformation of aeolian facies: the Cretaceous Troncoso Member, Neuquen Basin, Argentina. Geol. Soc. London Spec. Publ 252, 163–183 (2005).

Stump, T. E. & J. G. Vandereem. THE STRATIGRAPHY, DEPOSITIONAL-ENVIRONMENTS AND PERIODS OF DEFORMATION OF THE WAJID OUTCROP BELT, SOUTHWESTERN SAUDI-ARABIA. JOURNAL OF AFRICAN EARTH SCIENCES 21(3), 421-441 (1995). https://doi.org/10.1016/0899-5362(95)00099-F

Sun, D., D. Liu, M. Chen, Z. An & S. John. Magnetostratigraphy and palaeoclimate of Red Clay sequences from Chinese Loess Plateau. Science in China Series D: Earth Sciences 40(4), 337-343 (1997). https://doi.org/10.1007/BF02877564

Swezey, C. S., M. Deynoux & D. Jeannette. Sandstone depositional environments of the Upper Permian Champenay Formation, Champenay Basin, northeastern France. Sed. Geol 105, 91–103 (1996).

Swezey, C. S. Revisiting the age of the Sahara desert. SCIENCE 312(5777), 1138-1139 (2006).

Swezey, C. S., K. G. Havholm, G. M. Krezoski & J. E. Marzolf. Mississippian (Chesterian) eolian strata in the eastern united States. Southeastern Section. 61st Annual Meeting. Geol. Soc. Am. Ab. Progr 44, 13 (2012).

Szigeti, G. J. & J. E. Fox. Unkpapa Sandstone (Jurassic), Black Hills, South Dakota. An eolian facies of the Morrison Formation. Recent and ancient nonmarine depositional environments: models for exploration 31, 331–249 (1981).

Tanner, L. H. & J. F. Hubert. Depositional facies, paleogeography and paleoclimatology of the Lower Jurassic McCoy Brook Formation, Fundy Rift Basin, Nova-Scotia. Palaeogeogr. Palaeoclimatol. Palaeoecol 96, 261–280 (1992).

Tanner, L. H. & S. G. Lucas. The Moenave Formation: Sedimentologic and stratigraphic context of the Triassic-Jurassic boundary in the Four Corners area, southwestern USA. PALAEOGEOGRAPHY PALAEOCLIMATOLOGY PALAEOECOLOGY 244(1-4), 111-125 (2007). https://doi.org/10.1016/j.palaeo.2005.06.039

Tedesco, W. A., R. P. Major & L. R. Baria. An eolian facies within the Upper Jurassic Smackover Formation, Tchula Lake field, Mississippi. AAPG Bull 86, 485–503 (2002).

Tedford, R. H., J. B. Swinehart, C. C. Swisher, D. R. Prothero, S. A. King & T. E. Tierney (1996). The Terrestrial Eocene-Oligocene Transition in North America: The Whitneyan-Arikareean transition in the High Plains.

Tesón, E., E. L. Pueyo, A. Teixell, A. Barnolas, J. Agustí & M. Furió. Magnetostratigraphy of the Ouarzazate Basin: Implications for the timing of deformation and mountain building in the High Atlas Mountains of Morocco. GEODINAMICA ACTA 23(4), 151-165 (2010). https://doi.org/10.3166/ga.23.151-165

Thiry, M. D., M. B. Ayrault & J.-C. Grisoni. Ground-water silicification and leaching in sands: Example of the Fontainebleau Sand (Oligocene) in the Paris Basin. GSA Bulletin 100(8), 1283-1290 (1988). https://doi.org/10.1130/0016-7606(1988)100<1283:GWSALI>2.3.CO;2

Thornton, D. A. A potential aeolian oil reservoir: the Mid Devonian Tandalgoo Formation, Canning Basin. Depositional models and diagenesis. University of Adelaide. National Centre for Petroleum Geology and Geophysics. M.Sc. Thesis. (1990).

Trewin, N. H. & M. F. Thirlwall. Old Red Sandstone. The Geology of Scotland, Geological Society of London: 0 (2002).

Tripaldi, A. & C. O. Limarino. Vallecito Formation (Miocene): The evolution of an eolian system in an Andean foreland basin (northwestern Argentina). JOURNAL OF SOUTH AMERICAN EARTH SCIENCES 19(3), 343-357 (2005). https://doi.org/10.1016/j.jsames.2005.04.006

Tyrrell, S., S. Leleu, A. K. Souders, P. D. W. Haughton & J. S. Daly. K-feldspar sand-grain provenance in the Triassic, west of Shetland: distinguishing first-cycle and recycled sediment sources? GEOLOGICAL JOURNAL 44(6), 692-710 (2009). https://doi.org/10.1002/gj.1185

Uba, C. E., C. Heubeck & C. Hulka. Facies analysis and basin architecture of the Neogene Subandean synorogenic wedge, southern Bolivia. SEDIMENTARY GEOLOGY 180(3-4), 91-123 (2005). https://doi.org/10.1016/j.sedgeo.2005.06.013

Umhoefer, P. J., R. J. Dorsey, S. Willsey, L. Mayer & P. Renne. Stratigraphy and geochronology of the Comondu Group near Loreto, Baja California sur, Mexico. SEDIMENTARY GEOLOGY 144(1-2), 125-147 (2001). https://doi.org/10.1016/S0037-0738(01)00138-5

Veiga, G. D. & L. A. Spalletti. The Upper Jurassic (Kimmeridgian) fluvial-aeolian systems of the southern Neuquen Basin, Argentina. GONDWANA RESEARCH 11(3), 286-302 (2007). https://doi.org/10.1016/j.gr.2006.05.002

Voss, R. Cenozoic stratigraphy of the southern Salar de Antofalla region, northwestern Argentina. REVISTA GEOLOGICA DE CHILE 29(2), 167-189 (2002).

Weinberger, G. Investigation of grain size textural data as a parameter of dynamic depositional processes in the Lower Cretaceous Hatira Formation, Maktesh Gadol Masters Thesis, Ben Gurion University of the Negev (1980).

Xie, Y., D. J. Lunt & P. J. Valdes. Diagnosing the controls on desert dust emissions through the Phanerozoic. Climate of the Past 20(11), 2561-2585 (2024). https://doi.org/10.5194/cp-20-2561-2024

Xu, Y., L. Yue, J. Li, L. Sun, B. Sun, J. Zhang, et al. An 11-Ma-old red clay sequence on the Eastern Chinese Loess Plateau. Palaeogeography, Palaeoclimatology, Palaeoecology 284(3), 383-391 (2009). https://doi.org/https://doi.org/10.1016/j.palaeo.2009.10.023

Zavala, C. & R. H. Freije. On the understanding of aeolian sequence stratigraphy: An example from Miocene-Pliocene deposits in Patagonia, Argentina. RIVISTA ITALIANA DI PALEONTOLOGIA E STRATIGRAFIA 107(2), 251-264 (2001). https://doi.org/10.54103/2039-4942/16129

Zhang, Y., D. Sun, Z. Li, F. Wang, X. Wang, B. Li, et al. Cenozoic record of aeolian sediment accumulation and aridification from Lanzhou, China, driven by Tibetan Plateau uplift and global climate. Global and Planetary Change 120, 1-15 (2014). https://doi.org/https://doi.org/10.1016/j.gloplacha.2014.05.009

Zhu, Y., L. Zhou, D. Mo, A. Kaakinen, Z. Zhang & M. Fortelius. A new magnetostratigraphic framework for late Neogene Hipparion Red Clay in the eastern Loess Plateau of China. Palaeogeography, Palaeoclimatology, Palaeoecology 268(1), 47-57 (2008). https://doi.org/https://doi.org/10.1016/j.palaeo.2008.08.001